Journal of Photochemistry and Photobiology 6 (2021) 100025

Contents lists available at ScienceDirect

Journal of Photochemistry and Photobiology

journal homepage: www.elsevier.com/locate/jpap

The oxidation of guanine by photoionized 2-aminopurine

Graham D. Bull, Katherine C. Thompson*

Institute of Structural and Molecular Biology, Department of Biological Sciences, Birkbeck, University of London, Malet Street, London, WC1E 7HX, UK

ARTICLE INFO

Keywords:
Charge transfer
Radical cation
Radical anion
Neutral radical
Deprotonation

ABSTRACT

2-Aminopurine (2AP) is a fluorescent nucleobase analogue of the DNA nucleobase adenine and can be inserted in place of adenine into nucleic acids with minimal structural perturbation. The inserted 2-aminopurine can be selectively excited, and the fluorescence observed used as a sensitive probe for local structure, in addition selective ionization of 2-aminopurine within a nucleic acid is possible and once formed the ionized 2-aminopurine will oxidize nearby guanine bases, providing a route to study charge transfer within nucleic acids. Time resolved infrared spectroscopy is a powerful tool to study oxidation processes on picosecond, and longer timescales. There is a lack of availability of high quality IR spectra in the literature of the individual, short lived, photoproducts, required to fully elucidate the mechanism of the interaction of photoionized 2-aminopurine with guanine. Density functional theory (DFT) methods (B3LYP/6–31G+(d) and EDF1/6–31G+(d)) have been used to calculate the energies and infrared spectra of 2-aminopurine, guanine and potential photoproducts that may result from photoionization reactions between 2-aminopurine and guanine. Direct comparison can therefore be made between areas of bleaching of bands in the IR spectra of 2-aminopurine or guanine and the appearance of new transient bands of potential photoproducts. These potential photoproducts could include deprotonated neutral radical species, deprotonated anion species, radical cations and radical anions. It was found in the current work that the key intermediates in the oxidation reaction between photoionized 2-aminopurine and guanine were: 2AP•(−*H*,N2) (formed from deprotonation from the $2AP^{\bullet+}$ amino group); G•(−*H*) (formed from deprotonation from the N1 nitrogen, or possibly the amino group, of the initially formed $G^{\bullet+}$), and $2AP^{-}$(−*H*,N2) (formed from the reduction of 2AP•(−*H*,N2) by guanine).

1. Introduction

Solar UV radiation absorbed by DNA can cause damage to the DNA leading to mutations, the onset of cancer, oxidative stress and inflammation [14,15,32]. In cells, one-electron oxidation of the four natural DNA bases can lead to the formation of DNA base radicals, with guanosine having the lowest ionization potential [43,86] and the lowest aqueous solution oxidation potential [100,118]. One-electron oxidation of guanine in aqueous solution produces the guanine radical cation ($G^{\bullet+}$), whose chemistry is extensively documented in the literature [12,48]. Experimental studies of $G^{\bullet+}$ using widely differing techniques include: direct monophotonic ionization from 193 nm laser pulses [18,70,71], direct biphotonic laser irradiation using high-intensity 248 nm and 266 nm laser pulses [4,22,26,27,77], UV–vis spectra after pulse radiolysis [6,17,20,53,54,61,115,117], electron spin resonance (ESR) spectroscopy [1,3,7,41,92,102], cyclic voltammetry [52,63], laser flash photolysis [9,62,94,95,107,119,126], transient absorption spectroscopy [8,40], vibrational spectroscopy [87,124,128,134], transient infrared spectroscopy [134], mass spectrometry after electrospray ionization (ESI) [30], and theoretical methods [1,3,30,44,58]. The structure of guanine is shown in Scheme I.

$G^{\bullet+}$ is a Brønsted acid with a pKa = 3.9 (pKa for deoxyguanosine = 9.4) in neutral aqueous solution [6,17,115], thus the guanine radical cation is isolated only under acidic conditions with a lifetime of ~3 ms in aqueous solution with a pH ≤ 2.5 [94]. Under such conditions hydration reactions take place to form 8–oxo–7,8-dihydroguanosine (8–oxoG). At neutral pH levels (pH ≈ 7), $G^{\bullet+}$ undergoes deprotonation to form the neutral guanine radical, G•(−*H*), with a lifetime of ~70 ms at pH = 8 [94]. The deprotonated guanine radical G•(−*H*) does not easily undergo hydrolysis, but instead reacts with dioxygen to form a variety of imidazolone and oxazolone products [12,13,47,73,14,32,95].

Deprotonation of the guanine radical cation, $G^{\bullet+}$ could potentially occur by loss of a proton from either the N1, N2, N2' or C8 positions [103,105,106,108]. The preferred site of deprotonation is proposed to be from the guanine N1 position [1,2,17,58,92,115]. However, a contrasting view was proposed by Hole et al. [41] using ESR and ENDOR spectroscopy who argued in favour of deprotonation from the NH_2 group of $G^{\bullet+}$. Adhikary et al. [3] found proton release from the N1 or N2 position of $G^{\bullet+}$ to be temperature sensitive.

* Corresponding author.
E-mail addresses: k.thompson@bbk.ac.uk, thompson@mail.cryst.bbk.ac.uk (K.C. Thompson).

https://doi.org/10.1016/j.jpap.2021.100025
Received 14 September 2020; Received in revised form 1 March 2021; Accepted 1 March 2021
Available online 7 March 2021

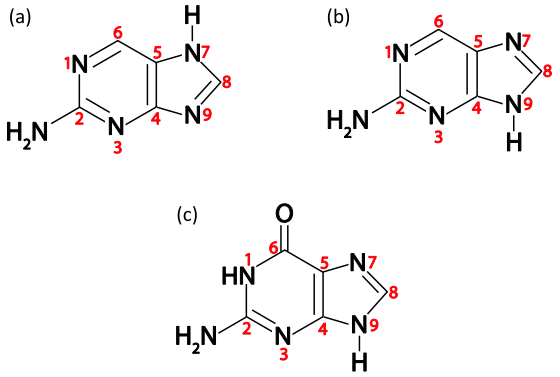

Scheme I. Numbering and atom labelling for: (a) 7H–2-Aminopurine (7H–2AP), (b) 9H–2-Aminopurine (9H–2AP), and (c) Guanine (G).

The rate of deprotonation from $G^{\bullet+}$ into the solvent is faster for the guanine monomer and single-stranded DNA (ssDNA) than in double-stranded DNA (dsDNA) [53,54]. In ssDNA deprotonation of $G^{\bullet+}$ is kinetically favoured (taking place over several seconds) over hydration of $G^{\bullet+}$ which results in producing 8–oxoG [95]. However, the formation of 8–oxoG becomes more kinetically favourable in dsDNA than in ssDNA [4,47,124]. This is attributed to the guanine radical retaining more of its cationic character in dsDNA than in ssDNA. In dsDNA, $G^{\bullet+}$ can react in two different ways, firstly, by hydration to form 8–oxoG and, secondly, deprotonation to the solvent to form the [G(–*H*)•:C] base pair which does not undergo further reactions with water [95].

It has long been known that DNA damage is more prone to occur at GG and GGG sites than at sites of isolated guanine [5,35,37,62,96,97,103]. Gasper and Schuster [35] used a 5′–end-capping quinone to introduce charge into a 25-mer DNA sequence. Irradiation at 350 nm, followed by treatment with piperidine results in strand cleavage at 5′–G of the distal GG-doublet which is more than 40 Å away from the anthraquinone group. These results have been interpreted in terms of the migration of a radical cation (electron hole) from the point of generation near the anthraquinone, transported along the duplex DNA to its point of reaction mostly at the 5′–G of the GG steps [35]. Several authors, [5,39,45,80,89,97,101] have also observed that reactivity is higher at the 5′–G end than at the 3′–G end of GG-doublets when the base at the 3′– position is cytosine or thymine. Where adenine is at the 3′– position, both the 5′– and 3′– guanines are oxidized.

Ward et al. [125] reported that 2-aminopurine, a structural isomer of the base adenine (6-aminopurine), was highly fluorescent and could be selectively excited in the presence of natural nucleotide bases. 2-Aminopurine (2AP) has two major tautomers, 9H–2AP and 7H–2AP (as shown in Scheme I) which exist in aqueous solutions in a 60:40 ratio, respectively [75]. When 2AP is incorporated into a nucleic acid only the 9H tautomeric form need be considered, but if experiments are performed with the free base the presence of both tautomeric forms must be considered. Other properties of 2AP are an excitation maximum of 305 nm [112] which is red-shifted compared to adenine which has an excitation maximum at a wavelength of 260.5 nm [16,123]. 2-Aminopurine generally has minimal perturbation to the structure of a nucleic acid when it is substituted for adenine as they are both structurally similar, and can form a Watson-Crick base pair with thymine in DNA and uracil in RNA [28,114]. One of the most useful properties of 2AP is the quenching of its fluorescence when it is incorporated in single-stranded nucleic acid and in double-stranded nucleic acid the fluorescence of 2AP is quenched further still [93,125]. Fluorescence quenching of 2AP in DNA has been attributed to DNA stacking interactions, hydrogen bonding, collisional interactions and charge transfer processes between the DNA nucleobases and electronically excited 2AP and this property has been applied in the study of charge transfer dynamics in DNA [31,46,51,59,60,81,82,83,84,85,90,103,113,133].

The low energy absorption maximum of 2AP allows selective and direct excitation when it is incorporated within a synthetic DNA sequence [42]. The use of intense light from a pulsed laser source can result in biphotonic absorption which results in photoionization of 2AP to form a radical cation, $2AP^{\bullet+}$and a solvated electron, e_h^- [17,18,116]. The solvated electron may then react with molecular oxygen, O_2, if present, which efficiently removes solvated electrons from the chemical system with a rate constant of $k = 1.9 \times 10^{10}$ L mol^{-1} s^{-1} [11,17,18,115]. Once formed, the $O_2^{\bullet-}$ radical anion is relatively unreactive towards $2AP^{\bullet+}$, but can react with 2AP•(–*H*) radicals, which decay on a ~100 μs time scale with the possible formation of hydroperoxides [104]. The 2AP radical cation ($2AP^{\bullet+}$) is a Brønsted acid with a p*K*a = 2.8 ± 0.2 [104], which rapidly deprotonates from one of a number of possible positions (which for the N9 tautomer are N2, N2', C6, or C8) to form neutral 2AP•(-H) radicals.

It was shown by Shafirovich et al. [103] that 2AP•(–*H*) is capable of oxidising guanine but not the other DNA bases, adenine, cytosine and thymine [36,66,75,103–107,118,129]. Thus, it was proposed that two photon absorption of 2AP leads to $2AP^{\bullet+}$, which deprotonates to form 2AP•(–*H*), which in turn can oxidise guanine, leading to the reformation of 2AP. The oxidised guanine will deprotonate such that G•(–*H*) is produced. When 2AP is present in an oligomer of DNA containing more than one guanine residue the preference for oxidation of different guanines may be predicted. Misiaszek et al. [73] have suggested G•(–*H*) can undergo a reaction with the $O_2^{\bullet-}$ radical anion at the C_5 (carbon centred radical) position with a rate constant of 3×10^9 M^{-1} s^{-1} [19]. This is the first step in a complicated reaction sequence described by Misiaszek et al. [73] that leads to the formation of an end product, 2,2,4–triamino–5(2*H*)–oxazolone.

From the preceding discussion it can be seen there has been extensive spectroscopic work examining the fate of the guanine radical cation ($G^{\bullet+}$) and the neutral guanine radical G•(–*H*) in DNA and to a lesser extent for the radical ions of 2-aminopurine. However, the system is still not completely understood. The majority of experiments involve exploring the UV/visible absorption spectra of the reaction mixtures. There is a paucity in the use of vibrational spectra to understand the excited state chemical, photophysical and photochemical processes and their effect upon biological activity of the nucleic acid bases of DNA. Examples where vibrational spectroscopy has been utilised in the study of DNA nucleobases include areas such as their vibrational modes [79,34], tautomerism [21,38,74,78,99], hydrogen bonding [33,10]; and interaction of the nucleic acid bases with H_2O clusters [64,110,111].

More recently, techniques using time-resolved infrared (TRIR) measurements on picosecond or femtosecond time scales [122] have been used by various spectroscopists in order to investigate the ultrafast processes which take place in polynucleotide DNA, individual nucleic acid bases and nucleobase analogues such as 2-aminopurine. TRIR can be used to provide detailed structural information of transient species and also to monitor the relaxation process after initial excitation. The variety of structures and systems studied using TRIR methods include the B and Z forms of $[poly(dG–dC)]_2$ [24], the interaction of $[Ru(phen)_2(dppz)]^{2+}$ with DNA [88], cytosine rich i-motif structures [50], the nucleotide 5′–GMP and polynucleotides poly[(dGdC)•poly(dGdC)] and [poly(G)] [56,68], stacked G-tetrad structures [67], chemistry of the guanine radical cation $G^{\bullet+}$ [87], the dinucleotide composed of 5′–8–oxoguanine anion and neutral 3′–adenine,[130] the formation of the 2AP radical cation $2AP^{\bullet+}$ and its subsequent deprotonation to form the neutral radical 2AP•(–*H*) [57], 1-methylcytosine and 5′–dCMP [49], thymine and thymidine [131], the Flavin chromophore [55], and stacked adenine–thymine systems [25].

Whilst TRIR is a powerful technique in its ability to record the changes that take place during the rapid processes associated with the ultrafast electronic and energetic perturbations that follow photon absorption. Identifying the nature of transient products is difficult without access to reliable calculated infrared spectra. In this paper we present energies and calculated infrared spectra for 2-aminopurine, its radical

Table 1
Structures of the potential photoproducts of 9H-2-aminopurine, 7H-2-aminopurine and guanine considered in this work. Equilibrium geometries energies and vibrational frequencies were calculated. Numbers in brackets refer to positions where a proton has been lost from a carbon atom or from a nitrogen atom.

7H–2-Aminopurine potential photoproducts		9H–2-Aminopurine potential photoproducts		Guanine and potential photoproducts	
2AP•(–H,N2)	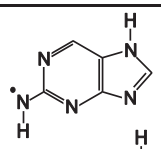	2AP•(–H,N2)	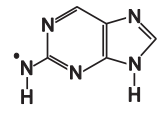	G•(–H,N1)	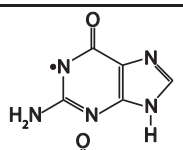
2AP•(–H,N2')	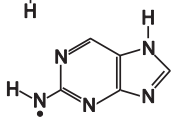	2AP•(–H,N2')	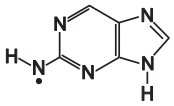	G•(–H,N2)	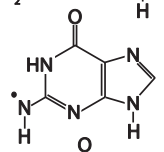
2AP•(–H,C6)	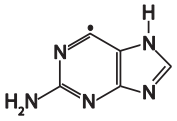	2AP•(–H,C6)	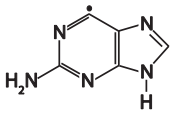	G•(–H.N2')	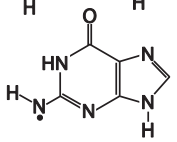
2AP•(–H,C8)	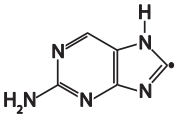	2AP•(–H,C8)	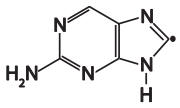	G•(–H,C8)	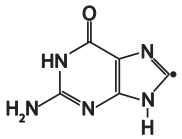
$2AP^{+\bullet}$	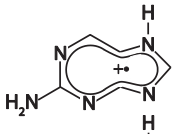	$2AP^{+\bullet}$	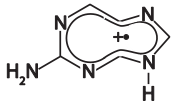	$G^{+\bullet}$	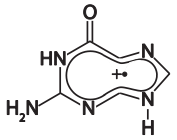
$2AP^{-\bullet}$	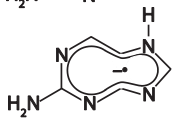	$2AP^{\bullet-}$	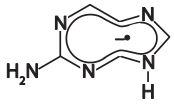		
$2AP^{-}(-H^{+},N2)$	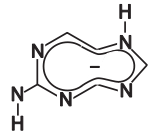	$2AP^{-}(-H^{+},N2)$	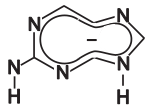		
$2AP^{-}(-H^{+},N2')$	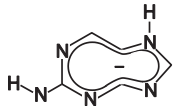	$2AP^{-}(-H^{+},N2')$	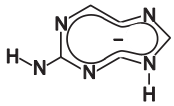		
$2AP^{-}(-H^{+},C6)$	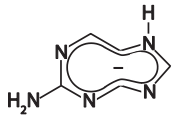	$2AP^{-}(-H^{+},C6)$	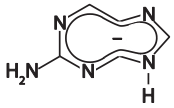		
$2AP^{-}(-H^{+},C8)$	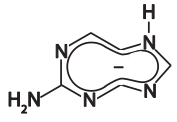	$2AP^{-}(-H^{+},C8)$	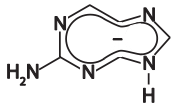		

anion, radical cation, deprotonated neutral radical structures and deprotonated anions. In the case of guanine, the infrared spectra of the radical cation and deprotonated neutral radical structures. The infrared spectra of 2-aminopurine and guanine are applied to the oxidation of guanine by photoexcited 2-aminopurine to highlight the spectroscopic signatures of the potential species involved.

2. Computational methods

Ground state (S_0) geometry optimization calculations were performed on each of 7H–2AP, 9H–2AP and guanine together with their respective predicted photoproducts as shown in Table 1 in order to find their optimised geometries, energies and related properties such as vibrational spectra. Geometry optimizations and frequency calculations were carried out using two density functional methods, B3LYP and EDF1 with the 6–31+*G*(d) basis set throughout. Previous studies [109,29,57,65,69,87,110,127,91] have demonstrated that the DFT methods B3LYP and EDF1 give good predictions of the geometries and vibrational frequencies of the nucleic acid bases and their analogues. No symmetry constraints were applied during geometry optimization. The intramolecular distances calculated by the B3LYP and EDF1 methods are within 0.021 Å and 0.030 Å, respectively, when compared to the crystal structure of 2AP•H_2O determined by Neely et al.[76]; for guanine, the B3LYP and EDF1 intramolecular distances are within 0.024 Å

Table 2a
Final electronic energies and zero point corrected electronic energies for the 7H and 9H tautomers of 2-aminopurine. Molecules are grouped according to charge and multiplicity with Δ*E* being the energy difference between the lowest energy photoproduct of each group (highlighted by 0.000 in table). Zero point energies have been scaled by 0.9636 [72] and calculations have been performed at B3LYP/6 − 31+*G*(d) level.

	9H-2AP			7H-2AP		
Molecule / Potential photoproduct	Electronic energy / Hartree	Sum of electronic energy and scaled ZPE / Hartree	Δ*E* / kcal mol^{-1}	Electronic energy / Hartree	Sum of electronic energy and scaled ZPE / Hartree	Δ*E* / kcal mol^{-1}
2AP	−467.09431	−466.98693	**0.00000**	−467.09246	−466.98564	0.81246
2AP•(−*H*,N2′)	−466.43601	−466.34073	**0.00000**	−466.43317	−466.33754	2.00030
2AP•(−*H*,N2)	−466.43554	−466.34031	0.26678	−466.43298	−466.33728	2.16789
2AP•(−*H*,C6)	−466.42062	−466.32541	9.61446	−466.41901	−466.32390	10.56077
2AP•(−*H*,C8)	−466.40308	−466.30822	20.40370	−466.40042	−466.30472	22.59705
2AP$^{\bullet+}$	−466.87965	−466.76918	**0.00000**	−466.87585	−466.76506	2.58600
2AP$^{\bullet-}$	−467.15940	−467.05517	0.34168	−467.15944	−467.05571	**0.00000**
2AP^{-}(−H^{+},N2')	−466.59551	−466.50028	0.52832	−466.59054	−466.49603	3.19364
2AP^{-}(−H^{+},N2)	−466.59516	−466.50112	**0.00000**	−466.59055	−466.49549	3.52950
2AP^{-}(−H^{+},C6)	−466.55256	−466.45808	27.00534	−466.55548	−466.46086	25.26140
2AP^{-}(−H^{+},C8)	−466.56868	−466.47393	17.06283	−466.56960	−466.47453	16.68255

and 0.048 Å, respectively, when compared to the crystal structure of guanine monohydrate [121]. Calculations in solution phase were completed using the polarizable continuum model. The software used for this work was GAMESS–US (General Atomic and Molecular Electronic Structure System) [98] version 12-JAN-2009 (R3). Each individual band was convoluted using a Lorentzian shape.

The existence of 2-aminopurine as two main tautomers (7H–2AP and 9H–2AP) in solution phase [75] needs to be accounted for if a single calculated IR spectra of free 2-aminopurine is to be presented. Calculating the expected ratio of 7H–2AP and 9H–2AP at equilibrium using the Boltzmann equation will enable a single calculated spectrum for 2AP to be determined with the expected contributions from 7H– and 9H–2AP tautomers.

The harmonic vibrational frequencies, performed at the minimum-energy geometries, calculated by electronic structure methods tend to be larger than the frequencies observed experimentally. Reasons why these discrepancies arise are due to the neglect of anharmonicity effects, and also because of incomplete incorporation of electron correlation and the use of limited basis sets [72]. The nature of the overestimation is usually uniform, and so for a particular theoretical procedure and basis set, generic frequency scale factors may be applied. For the present study the scale factors used for B3LYP are 0.9636 [72]. A scaling value for the EDF1 functional with the 6–31+*G*(d) basis set was not found in the literature. However, a value (0.9820) for EDF1 using the 6–31+*G*(d,p) basis set was published by Merrick et al. [72] and was the scaling factor used in this study.

3. Results

The molecules of 7H/9H 2-aminopurine and guanine, subjects of the current investigation, consist of 15 and 16 atoms, respectively. Deprotonated (−*H*/−H^{+}) structures are defined by subtracting a single proton from the amino (NH_2) group, the C6 or the C8 positions of 2-aminopurine (Table 1). For guanine, a single proton is removed from the amino group, the N1 or C8 positions (Table 1).

The zero point corrected (ZPE) electronic (B3LYP) energies of 2-aminopurine and guanine are shown in Tables 2a and 2b. The results presented in Tables 2a and 2b were calculated using the B3LYP functional and an identical pattern of relative energy differences are observed for the ZPE energies of 2-aminopurine and guanine calculated using the EDF1 functional (see Table S1 in supplementary information). From Table 2a it can be seen that the 9H– tautomer of 2AP is predicted to be the more stable, but with a significant fraction, around 20%, existing in the 7H– form in aqueous solution, in line with experimental observations. The 9H– form is predicted to be the dominant (around 99%) form following oxidation of 2AP to form 2AP$^{\bullet+}$, e.g. as formed following two photon absorption. Loss of a proton from 2AP, to yield 2AP^{-}(−H^{+}), or loss of a proton from 2AP$^{\bullet+}$ to form 2AP•(−*H*) (equivalent to overall loss of hydrogen from 2AP) are both predicted to occur by loss of a hydrogen from N2, as the 2AP^{-}(−H^{+}, N2) and 2AP•(−*H*, N2) tautomeric forms are substantially more favourable on thermodynamic grounds than loss of a proton from the other possible positions.

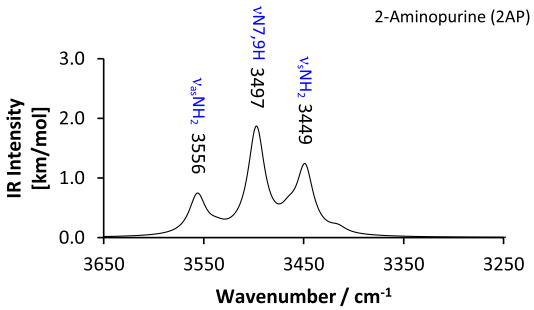

Fig. 1. Harmonic B3LYP/6 − 31+*G*(d) calculated IR spectra for 2-aminopurine (2AP) for the νNH_2 spectral region (3250 – 3650 cm^{-1}). Vibrational frequencies were calculated at B3LYP/6 − 31+*G*(d) level and scaled by 0.9636 [72]. 2-Aminopurine consists of a weighted mixture of 7H–2AP (12%) and 9H–2AP (88%). Assignments: ν_{as}, anti-symmetric stretching; ν, stretching; ν_s, symmetric stretching.

In the case of guanine, deprotonation of G$^{\bullet+}$ to form G•(−*H*) from the N1 position is found to be only slightly more favourable than loss from the N2 position. The two species G•(−*H*, N1) and G•(−*H*, N2) are expected to be present in the ratio of 60:40 at equilibrium at room temperature. Comparing the difference in energy between 2AP/2AP$^{\bullet+}$/2AP•(−*H*) with G/G$^{\bullet+}$/G•(−*H*) it can be seen that the oxidation of G by 2AP•(−*H*)$^{+}$ to form G•(−*H*) and 2AP is favourable, again, in agreement with experimental findings [103].

3.1. Interpretations of IR spectra

The nomenclature used to describe vibrational modes is as follows: ν, stretching; ν_s, symmetric stretch; ν_{as}, asymmetric stretch; β, in-plane bending; γ, out-of-plane bending; σ, scissoring; ω, wagging; δ, rocking; τ, torsion. The detailed descriptions for the vibrational assignments of 2-aminopurine and guanine are summarised in the following sections.

3.2. NH_2 vibrations

Fig. 1 shows the B3LYP calculated IR spectra of 2AP in the νNH_2 stretch spectral region (3250 – 3650 cm^{-1}). Three sharp bands are

Table 2b
Final electronic energies and zero point corrected electronic energies for guanine. Molecules are grouped according to charge and multiplicity with ΔE being the energy difference between the lowest energy photoproduct of the G•(−*H*) group (highlighted by 0.000 in table). Zero point energies have been scaled by 0.9636 [72] and calculations have been performed at B3LYP/6 − 31+*G*(d) level.

Molecule / Potential photoproduct	Electronic energy / Hartree	Sum of electronic energy and scaled ZPE / Hartree	ΔE / kcal mol^{-1}
G	−542.31733	−542.20495	**0.00000**
G•(−*H*,N1)	−541.66823	−541.56805	**0.00000**
G•(−*H*,N2′)	−541.66760	−541.56769	0.22870
G•(−*H*,N2)	−541.66334	−541.56283	3.27650
G•(−*H*,C8)	−541.62534	−541.52511	26.94388
G$^{\bullet+}$	−542.10713	−541.99130	**0.00000**

Table 3
Vibrational modes and frequencies (in cm^{-1}) of 2-aminopurine, guanine and their potential photoproducts in the NH_2 spectral range (3250 - 3650 cm^{-1}). Vibrational frequencies were calculated at B3LYP/6 − 31+*G*(d) and EDF1/6 − 31+*G*(d) levels and are scaled by 0.9636 and 0.9820, respectively [72]. Experimental data is taken from [a]Seefeld et al. [99] and [b]Szczepaniak and Szczesniak [120]. Assignments: ν_{as}, anti-symmetric stretching; ν, stretching; ν_s, symmetric stretching.

2AP Potential Photoproducts	**B3LYP**			**EDF1**		
	$\nu_{as}NH_2$	$\nu N_{7,9}H$	$\nu_s NH_2$	$\nu_{as}NH_2$	$\nu N_{7,9}H$	$\nu_s NH_2$
2AP	3556 (3579)[a]	3497 (3508)[a]	3449 (3463)[a]	3571	3521	3457
2AP•(−*H*,N2)		3498			3521	
2AP•(−*H*,N2′)		3499			3519	
2AP•(−*H*,C6)	3573	3491	3462	3593	3522	3461
2AP•(−*H*,C8)	3533	3513	3422	3587	3537	3457
2AP$^{\bullet+}$	3508	3499	3377	3576	3521	3461
2AP$^{-\bullet}$	3499	3510	3404	3521	3511	3423
2AP^{-}(−H^+,N2)		3504			3524	
2AP^{-}(−H^+,N2′)		3516			3534	
2AP^{-}(−H^+,C6)	3517	3484	3413	3531	3494	3424
2AP^{-}(−H^+,C8)	3527	3521	3422	3554	3505	3450
Guanine Potential Photoproducts	**B3LYP**			**EDF1**		
	$\nu_{as}NH_2$	νN_9H	$\nu_s NH_2$	$\nu_{as}NH_2$	νN_9H	$\nu_s NH_2$
G	3559 (3570)[b]	3493 (3493)[b]	3457 (3455)[b]	3578	3514	3472
G•(−*H*,N1)	3581	3502	3461	3612	3519	3488
G•(−*H*,N2)		3503			3525	
G•(−*H*,N2′)		3493			3515	
G•(−*H*,C8)	3576	3511	3472	3596	3528	3490
G$^{\bullet+}$	3529	3492	3417	3563	3517	3444

shown at 3556 cm^{-1}, 3597 cm^{-1} and 3449 cm^{-1} which are in the order of the asymmetric NH_2 ($\nu_{as}NH_2$) stretch, the free νN7,9H stretch and the symmetric NH_2 ($\nu_s NH_2$) stretch, respectively. **Table 3** lists the B3LYP and EDF1 scaled harmonic vibrational frequencies for 2-aminopurine and potential 2AP photoproducts. The scaled B3LYP (0.9636) and EDF1 (0.9820) frequencies for the νN7,9H stretch are underestimated by 11 cm^{-1} and overestimated by 13 cm^{-1} compared to experimental values [99], respectively. Similarly, the scaled B3LYP calculated $\nu_{as}NH_2$ and $\nu_s NH_2$ stretches are underestimated by 23 cm^{-1} and 14 cm^{-1}, respectively and underestimated by 8 cm^{-1} and 6 cm^{-1}, respectively when calculated using EDF1.

The free νN7,9H stretch is common to all potential 2-aminopurine photoproducts (Table 3) and are reasonably consistent in frequency with a range of 3494–3521 cm^{-1}. In those potential 2AP photoproducts where a proton has been removed from the amino group only two peaks are observed, the free νN7,9H stretch and the free NH stretch of the former amino group.

The scissoring NH_2 vibrational mode (σNH_2) is characteristic to all photoproducts of 2-aminopurine (except for those 2-aminopurine photoproducts where a proton has been removed from the amino (NH_2) group) with a harmonic frequency range 1593–1688 cm^{-1} (Table 4). After scaling, the calculated B3LYP (σNH_2 = 1604 cm^{-1}) and EDF1 (σNH_2 = 1600 cm^{-1}) values are in excellent agreement with experiment, overestimating the experimental value [99] by 10 cm^{-1} and 6 cm^{-1}, respectively.

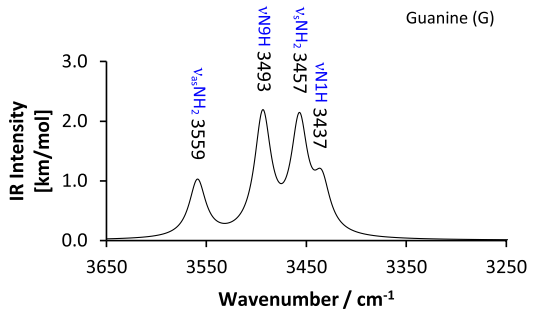

Fig. 2. Harmonic B3LYP/6 − 31+*G*(d) calculated IR spectra for guanine (G) for the νNH_2 spectral region (3250 – 3650 cm^{-1}). Vibrational frequencies were calculated at B3LYP/6 − 31+*G*(d) level and scaled by 0.9636. Assignments: ν_{as}, anti-symmetric stretching; ν, stretching; ν_s, symmetric stretching.

The calculated spectra for guanine over the NH_2 spectral region 3250–3650 cm^{-1} is shown in Fig. 2. Four spectral bands are observed, in order of decreasing frequency the asymmetric NH_2 ($\nu_{as}NH_2$) stretch, the free νN9H stretch, the symmetric NH_2 ($\nu_s NH_2$) stretch and the free νN1H stretch. The scaled B3LYP calculated frequencies for these bands are 3559 cm^{-1}, 3494 cm^{-1}, 3457 cm^{-1} and 3435 cm^{-1}, respectively. Experimental frequencies measured by Szczepaniak and Szczesniak [120] for

Table 4
Vibrational frequencies (in cm^{-1}) of 2-aminopurine, guanine and their potential photoproducts for the scissoring σNH_2 vibrational mode. Vibrational frequencies were calculated at B3LYP/6 − 31+*G*(d) and EDF1/6 − 31+*G*(d) levels and are scaled by 0.9636 and 0.9820, respectively [72]. Experimental data is taken from [a]Seefeld et al. [99] and [b]Szczepaniak and Szczesniak [120]. Note that the tautomers 2AP•(−*H*,N2) and G•(−*H*,N2) cannot have a scissoring σNH_2 vibrational mode due to the absence of the amino group.

2-Aminopurine Photoproducts	**B3LYP** σNH_2	**EDF1** σNH_2
2AP	1604 (1594)[a]	1600
2AP•(−*H*,N2)	–	–
2AP•(−*H*,C6)	1626	1629
2AP•(−*H*,C8)	1606	1611
$2AP^{\bullet+}$	1688	1700
$2AP^{-\bullet}$	1590	1601
$2AP^{-}$(−H^{+},N2)	–	–
$2AP^{-}$(−H^{+},C6)	1573	1629
$2AP^{-}$(−H^{+},C8)	1598	1607
Guanine Photoproducts	**B3LYP** σNH_2	**EDF1** σNH_2
G	1602 (1629–1654)[b]	1601
G•(−*H*,N1)	1456–1587	1452–1575
G•(−*H*,N2)	–	–
G•(−*H*,C8)	1642–1662	1641–1664
$G^{\bullet+}$	1649	1647

the $\nu_{as}NH_2$, the free νN9H, the $\nu_{s}NH_2$ and the free νN1H stretches are 3526–3570 cm^{-1}, 3493 cm^{-1}, 3428–3455 cm^{-1} and 3439 cm^{-1}, respectively. As was observed with 2AP, the νN9H stretch is ubiquitous to the potential photoproducts of guanine and is generally consistent within a frequency range of 3492–3511 cm^{-1}. The B3LYP scaled harmonic frequencies are in excellent agreement with experiment (Table 3) [120]. The asymmetric NH_2 ($\nu_{as}NH_2$) stretch underestimates the experimental value [120] by 11 cm^{-1}, the free νN9H stretch is predicted to be near identical to the experimental value [120] and both the symmetric NH_2 ($\nu_{s}NH_2$) and free N1H stretches underestimate the experimental frequencies [120] by 2 cm^{-1}.

The second major type of NH_2 vibrational mode of guanine is due to scissoring NH_2 (σNH_2). The experimental frequency of this mode is 1629–1654 cm^{-1} [120]. The scaled (Table 4) frequencies calculated by B3LYP (σNH_2 = 1602 cm^{-1}) and EDF1 (σNH_2 = 1601 cm^{-1}) underestimate the experimental frequencies [120] by at least 27 cm^{-1}.

3.3. CO vibrations

The heterocyclic aromatic carbonyl stretch (νCO) is the most distinctive vibrational mode of guanine. Fig. 3 show the B3LYP calculated spectra of guanine in the νCO spectral range (1500–1750 cm^{-1}). The scaled B3LYP and EDF1 calculated νCO stretch for guanine is 1653 cm^{-1} and 1657 cm^{-1}, respectively. Szczepaniak and Szczesniak [120] determined a range (νCO = 1692–1749 cm^{-1}) of experimentally measured values for the guanine νCO stretch. Similarly, Delabar and Majoube [23] recorded an experimental guanine νCO stretch of 1702 cm^{-1}. The scaled B3LYP (νCO = 1653 cm^{-1}) and EDF1 (νCO = 1657 cm^{-1}) calculated values underestimate the experimental value of Delabar and Majoube [23] by 49 cm^{-1} and 45 cm^{-1}, respectively. Table 5 shows the B3LYP and EDF1 calculated scaled harmonic frequencies for νCO and stretching frequencies of guanine and the potential photoproducts of guanine.

3.4. In-plane purine ring vibrations

In-plane ring vibrations are observed in three distinct regions of the IR spectrum of the photoproducts of 2-aminopurine and guanine. The first region is dominated by low to very high intensity in-plane ring vibrations in the spectral range 1072–1637 cm^{-1} for 2-aminopurine and 1312–1558 cm^{-1} for guanine. The second region, 743–1104 cm^{-1}, for the photoproducts of 2-aminopurine and 771–1585 cm^{-1} for the photoproducts of guanine consist of a mixture of generally low intensity bands of in plane ring vibrations, $\nu CXNY$ / νCNH_2 stretching, δNH_2 rocking and ωCXH wagging modes. The third region (below 700 cm^{-1}), for both 2-aminopurine and guanine, is made up of a mixture of β-ring, γ-ring, δ-ring and τ-ring vibrations which are discussed in Section 3.7.

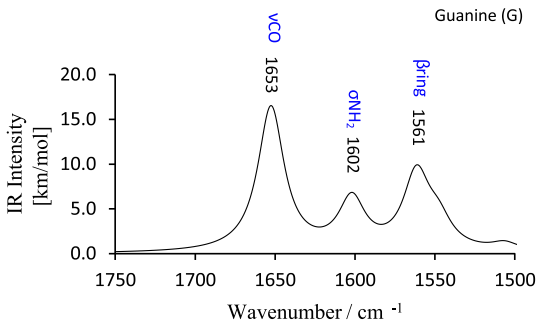

Fig. 3. Harmonic B3LYP/6 − 31+*G*(d) calculated IR spectra for guanine (G) for the νCO spectral region (1500 – 1750 cm^{-1}). Vibrational frequencies were calculated at B3LYP/6 − 31+*G*(d) level and scaled by 0.9636. Assignments: ν, stretching; σ, scissoring; β, in-plane bending.

Table 5
Vibrational frequencies (in cm^{-1}) of guanine and potential photoproducts for the νCO vibrational stretch. Vibrational frequencies were calculated at B3LYP/6 − 31+*G*(d) and EDF1/6 − 31+*G*(d) levels and are scaled by 0.9636 and 0.9820, respectively [72]. Experimental data is taken from [a]Szczepaniak and Szczesniak [120]. Oxidation of guanine to form $G^{\bullet+}$ is predicted to lead to a blue shift in the position of the *C* = *O* vibrational mode. Deprotonation of $G^{\bullet+}$ to form G•(−*H*) is predicted to lead to a significant red shift compared to G, if the hydrogen is lost from N1, whereas little change in the peak position compared to G is predicted if the N2 (or C8) hydrogen is lost.

Guanine Photoproducts	**B3LYP** νCO	**EDF1** νCO
G	1653 (1692–1749)[a]	1657
G•(−*H*,N1)	1548–1587	1539–1575
G•(−*H*,N2)	1657	1653
G•(−*H*,N2')	1652	1649
G•(−*H*,C8)	1642–1662	1641–1664
$G^{\bullet+}$	1684–1694	1671–1681

3.5. CN vibrations

There is a zone of low intensity calculated harmonic vibrational frequencies in 2-aminopurine that occupy a spectral range of approximately 800–1100 cm^{-1}. Whilst this region is dominated by in-plane ring vibrations, there are some bands (such as the νC8N9 and νC2N3 vibrational stretches) characterised by $\nu CXNY$ vibrational stretches (Table 6), which are consistent throughout the calculated IR response of 2-aminopurine and 2AP photoproducts. There is generally very good agreement in the frequencies calculated by the B3LYP and EDF1 methods.

The νC8N9 and νC8N7 are the most common vibrational stretches in the spectra of guanine and guanine photoproducts occurring in two bands, a higher frequency band between 1232–1377 cm^{-1} and a lower frequency band between 1057–1104 cm^{-1} (Table 7). The νCNH_2 vibrational stretch is restricted to guanine (1327 cm^{-1}) and $G^{\bullet+}$ (1411 cm^{-1}).

Table 6
Vibrational frequencies (in cm^{-1}) of 2-aminopurine and potential photoproducts for the *νCXNY* vibrational stretch. Vibrational frequencies were calculated at B3LYP/6 − 31+*G*(d) and EDF1/6 − 31+*G*(d) levels and are scaled by 0.9636 and 0.9820, respectively [72].

2-Aminopurine Photoproducts	B3LYP *νCXNY*	EDF1 *νCXNY*
2AP	νC8N9 (1048) νC2N3 (1072)	νC8N9 (931) νC8N9 (1048) νC2N3 (1048) νC2N1 (1056)
2AP•(−*H*,N2)	νC8N9 (1078) νC2N3 (1102)	νC8N9 (1082) νC2N3 (1089)
2AP•(−*H*,N2')	νC8N9 (1088) νC2N3 (1104)	νC2N3 (1085) νC8N9 (1103)
2AP•(−*H*,C6)	νC2N1 (938) νC8N9 (1040) νC2N3 (1065)	νC2N1 (934) νC2N3 (1056) νC8N9 (1065)
2AP•(−*H*,C8)	νC2N3 (1051) νC8N9 (1077)	νC2N1 (936) νC2N3 (1058) νC8N9 (1093)
$2AP^{\bullet+}$	νC2N3 (1045) νC8N9 (1101)	νC2N3 (1073) νC8N9 (1115)
$2AP^{-\bullet}$	νC2N3 (1012) νC8N9 (1046)	νC2N3 (1016) νC8N9 (1048) νC6N1 (1073)
$2AP^{-}$(−H^{+},N2)	νC8N9 (1041) νC2N3 (1074)	νC8N9 (1045) νC2N3 (1065)
$2AP^{-}$(−H^{+},N2')	νC8N9 (1046) νC2N3 (1087)	νC8N9 (1052) νC2N3 (1080)
$2AP^{-}$(−H^{+},C6)	νC8N7 (1093) νC2N3 (1077)	νC8N7 (1094) νC2N3 (1079)
$2AP^{-}$(−H^{+},C8)	νC8N9 (910) νC2N3 (1092)	νC8N9 (911) νC2N3 (1090)

Table 7
Vibrational frequencies (in cm^{-1}) of guanine and potential photoproducts for the *νCXNY* vibrational stretch. Vibrational frequencies were calculated at B3LYP/6 − 31+*G*(d) and EDF1/6 − 31+*G*(d) levels and are scaled by 0.9636 and 0.9820, respectively [72].

Guanine Photoproducts	B3LYP *νCXNY*	EDF1 *νCXNY*
G	νC8N9 (1347) νCNH_2 (1327) νC8N9 (1057)	νC8N9 (1346) νCNH_2 (1328) νC8N9 (1065)
G•(−*H*,N1)	νC8N7 (1243) νC6N1 (1240) νC8N9 (1087)	νC8N7 (1243) νC6N1 (1240) νC8N9 (1087)
G•(−*H*,N2)	νC8N7 (1244) νC6N1 (1176) νC8N9 (1096)	νC8N7 (1243) νC6N1 (1170) νC8N9 (1095)
G•(−*H*,N2')	νC8N9 (1377) νC5N7 (1335) νC6N1 (1185)νC8N9 (1077)	νC8N9 (1377) νC5N7 (1340) νC6N1 (1175) νC8N9 (1077)
G•(−*H*,C8)	νCNH_2 (1324) νC8N9 (1311) νC5N7 (1284) νC6N1 (1120) νC8N9 (1082)	νCNH_2 (1322) νC8N9 (1312) νC5N7 (1288) νC6N1 (1115) νC8N9 (1084)
$G^{\bullet+}$	νCNH_2 (1411) νC8N7 (1232) νC8N9 (1104)	νCNH_2 (1404) νC8N7 (1232) νC8N9 (1107)

Table 8
Vibrational frequencies (in cm^{-1}) of 2-aminopurine, guanine and their potential photoproducts for the wagging *ω*C6H and *ω*C8H vibrational modes. Vibrational frequencies were calculated at B3LYP/6 − 31+*G*(d) and EDF1/6 − 31+*G*(d) levels and are scaled by 0.9636 and 0.9820, respectively [72].

2-Aminopurine Photoproducts	B3LYP *ω*C6H(*ω*C8H)	EDF1 *ω*C6H(*ω*C8H)
2AP	932 (833)	915 (816)
2AP•(−*H*,N2)	935 – 943 (935 – 943)	920 – 927 (920 – 927)
2AP•(−*H*,N2')	927 (812)	916 (833)
2AP•(−*H*,C6)	(830)	(800)
2AP•(−*H*,C8)	935 – 941	896
$2AP^{\bullet+}$	995 (1090)	983 (1063)
$2AP^{-}$(−H^{+},N2)	925	904
$2AP^{-}$(−H^{+},N2')	925	905
$2AP^{-}$(−H^{+},C6)	(843)	(812)
$2AP^{-}$(−H^{+},C8)	914	893
Guanine Photoproducts	**B3LYP** *ω*C8H	**EDF1** *ω*C8H
G	822	802–804
G•(−*H*,N1)	922	890
G•(−*H*,N2)	931	908
G•(−*H*,N2')	912	879
$G^{\bullet+}$	992	971

3.6. CH vibrations

In 2-aminopurine the *ω*C6H mode is consistently observed in all species, except for those species where the C6H proton is absent and the *ω*C8H mode is observed instead (Table 8). The *ω*C6H mode has a consistent frequency range throughout the series of 2AP photoproducts, 914–943 cm^{-1} and 893–927 cm^{-1} at B3LYP and EDF1 levels, respectively. The exception to this is $2AP^{\bullet+}$ where the *ω*C6H mode is at a higher frequency (995 cm^{-1} and 983 cm^{-1} at B3LYP and EDF1 levels, respectively). The *ω*C8H mode in 2-aminopurine follows a similar pattern as for the *ω*C6H mode (Table 8). Frequency ranges are consistent between the different 2AP species (812–943 cm^{-1} and 800–927 cm^{-1} at B3LYP and EDF1 levels, respectively). $2AP^{\bullet+}$ has a higher *ω*C8H frequency, 1090 cm^{-1} and 1063 cm^{-1} at B3LYP and EDF1 levels, respectively.

The *ω*C8H vibrational mode is consistently observed in guanine and guanine photoproducts (except for G•(−H,C8) where the C8 proton is absent). Table 8 shows the calculated vibrational frequencies of the *ω*C8H vibrational wagging mode using the B3LYP and EDF1 methods. Szczepaniak and Szczesniak [120] report an experimental CH out-of-plane bending mode at 925 cm^{-1} for guanine, but the particular carbon atom which this mode refers to is unspecified.

3.7. Low frequency vibrations

The low frequency vibrations (< 800 cm^{-1}) of 2-aminopurine and guanine are dominated by a mixture of in plane ring vibrations, out of plane ring vibrations, rocking and torsion vibrations of the rings with low to high intensities (Table 9).

The ωNH_2 wagging vibration of 2-aminopurine, calculated using B3LYP and EDF1, is distinctive for those species where it is observed with moderate to high intensity (Table 9). At EDF1 level, the ωNH_2 wagging mode is also observed for 2-aminopurine at a slightly red-shifted frequency of 401 cm^{-1}. In the case of guanine, the ωNH_2 mode is predicted by EDF1 at 443 cm^{-1}, but not by B3LYP which predicts the rocking δNH_2 mode over the spectral range < 800 cm^{-1}.

4. Discussion

A chemical pathway describing the oxidation of guanine by photoexcited 2-aminopurine was given in the introduction to this paper, along with a list of potential photoproducts in Table 1. Absorption (λ = 310 nm) in a biphotonic process leads to the formation of the 2-aminopurine radical cation, $2AP^{\bullet+}$ [57]. The calculated energies for the species considered here support the mechanism that photoionization of 2AP will lead to the formation of 2AP•(−H), where the H has been lost from the N2 position. The 2AP•(−H) can oxidise a guanine residue to reform 2AP and give, after loss of a proton the neutral radical species

Table 9
Vibrational frequencies (in cm^{-1}) of 2-aminopurine, guanine and their potential photoproducts for vibrational frequencies ⟨800 cm^{-1} and with an intensity⟩ 0.00005 km/mol. Vibrational frequencies were calculated at B3LYP/6 − 31+*G*(d) and EDF1/6 − 31+*G*(d) levels and are scaled by 0.9636 and 0.9820, respectively [72]. Assignments: β, in-plane bending; γ, out-of-plane bending; ω, wagging; δ, rocking; τ, torsion.

2-Aminopurine Photoproducts	**B3LYP**			**EDF1**		
	β ring	γ ring	ω,δNH_2; ωNH; τ,δring; ωC*X*H*Y*	β ring	γ ring	ω,δNH_2; ωNH; τ,δring; ωC*X*H*Y*
2AP	472	774 413 326	444 (ωNH_2)	765		505 (ωN9H), 438 (δNH_2), 401 (ωNH_2)
2AP•(−*H*,N2)	473 753	400 548	710 (ωNH)	751	678 633 559 390	713 (ωNH), 472 (δring)
2AP•(−*H*,N2')	364	774 576 212	728 (ωNH) 693 (ωNH)		769 725 568	363 (δring)
2AP•(−*H*,C6)	741 328	462	531 (ωN7H) 376 (ωNH_2)	729	635 557	799 (ωC8H), 482 (δring), 382 (δNH_2), 328 (δNH_2)
2AP•(−*H*,C8)	758 597 480 334	574 445	387 (ωNH_2)	744	610	476 (δring), 395 (δNH_2), 335 (δring)
$2AP^{\bullet+}$	469 359	584	786 (ωN7H) 687 (ωN7H) 304 (τring)		758 570 302	691 (ωNH), 475 (δring), 360 (δNH_2)
$2AP^{-\bullet}$	748 476	701 643 546 392	436 (ωC6H) 337 (ωC6H) 225 (τring) 146 (τring) 123 (τring) 12 (δring)	733	573 135	395 (ωNH_2), 337 (ωNH_2), 320 (ωNH_2)
$2AP^{-}$(−H^{+},N2)	753 711 627 513	374 294 188	669 (ωNH) 10 (δring)		188	737 (ωC8H), 624 (δring), 509 (δring), 369 (ωN9H), 288 (ωC8H)
$2AP^{-}$(−H^{+},N2')	749 620 367	785 478	193 (τring) 150 (τring) 21 (δring)		794	737 (ωNH), 484 (ωN9H), 364 (τring)
$2AP^{-}$(−H^{+},C6)	618 597 461	781 734 384 152	323 (δring)		772 725 147	619 (ωNH_2), 595 (δNH_2), 469 (ωN7H), 370 (δNH_2), 328 (δNH_2)
$2AP^{-}$(−H^{+},C8)	800	772 715 643 528 417 336	597 (ωNH_2) 378 (ωNH_2)		766 719 651 531 499 214	618 (ωNH_2), 604 (ωNH_2), 383 (δNH_2), 322 (δNH_2), 11 (δring)
Guanine Photoproducts	**B3LYP**			**EDF1**		
	β ring	γ ring	ω,δNH; δ,τ,ωNH_2; ωCO; τ,ωring	β ring	γ ring	ω,δNH; δ,τ,ωNH_2; ωCO; τ,ωring
G	309	745 704 671 643 193	439 (ωNH)		737 698 660 635 193	443 (ωNH_2), 329 (δNH_2), 267 (δNH_2), 9 (δring)
G•(−*H*,N1)	666 636 461	746 544	340 (δNH_2) 253 (ωNH_2) 167 (ωCO) 89 (τring) 14 (ωring)	503	745 616 88	661 (δring), 337 (δNH_2), 248 (ωNH_2), 168 (ωCO), 12 (δring)
G•(−*H*,N2)	308	734 668 543	785 (ωNH) 367 (δNH) 205 (τring)		737 532	761 (ωNH), 667 (δring), 363 (δNH), 205 (τring)
G•(−*H*,N2')	512	757 662 602	440 (ωN7H) 191 (τring) 18 (ωring)	606	745	664 (ωNH), 475 (ωN9H), 194 (τring)
G•(−*H*,C8)		724 651 580	523 (τNH_2) 457 (ωNH_2) 424 (ωNH) 342 (δNH_2) 196 (τring)		713 187	645 (δring), 543 (ωN9H), 490 (ωN1H), 408 (ωNH_2), 363 (ωNH_2), 327 (δNH_2)
$G^{+\bullet}$	646	725 668 569	771 (ωNH) 698 (ωNH) 22 (τring)		745 728	694 (ωN9H), 643 (δring), 574 (ωNH), 23 (δring)

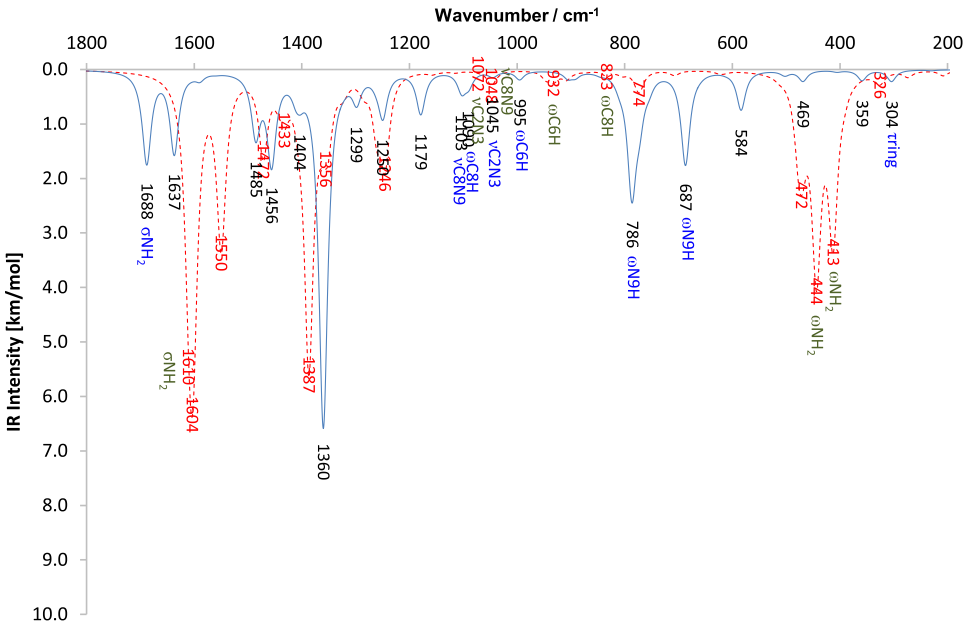

Fig. 4. Harmonic IR spectra of $2AP^{\bullet+}$ (solid blue line) and 2-aminopurine (dashed red line) calculated at B3LYP/6–31+*G*(d) level. B3LYP frequencies have been scaled by 0.9636 [72]. Annotation: ν, stretching; σ, scissoring; ω, wagging; τ, torsion. Vibrational frequencies without annotation are in-plane (βring) and out-of-plane (γring) ring vibrations. 2-Aminopurine consists of a weighted mixture of 7H–2AP (12%) and 9H–2AP (88%) and $2AP^{\bullet+}$ is a weighted mixture of 7H–2AP (2%) and 9H–2AP (98%).

G•(−H) from which the H may be lost from either the N1 or the N2 position of guanine. This appears to confirm the somewhat conflicting experimental data, where some had reported loss from N1, some N2 and some both [3,17,41,92]. The loss of a proton from the C8 position is not thermodynamically favourable, which may seem surprising given the importance of the C8 position of guanine in the formation of 8oxo–G.

The calculated spectra for $2AP^{\bullet+}$ (Fig. 4) show bands of 2-aminopurine (2AP) blue shifted by ~53–87 cm^{-1} upon formation of $2AP^{\bullet+}$. The spectral region of ~1550 cm^{-1} in 2AP appears to be bleached in $2AP^{\bullet+}$, with a blue shift (from 2AP → $2AP^{\bullet+}$) of the moderately intense σNH_2 (1610 cm^{-1} → 1688 cm^{-1}) and in-plane ring vibration (βring) (1604 cm^{-1} → 1637 cm^{-1}) bands are predicted with a much reduced intensity. Other notable shifts are νC8N9 1048 cm^{-1} → 1101 cm^{-1} and ωC6H 932 cm^{-1} → 995 cm^{-1}. At lower frequencies there is an appearance of low intensity transient bands at 786 cm^{-1}, 687 cm^{-1} and 584 cm^{-1} in the spectra of $2AP^{\bullet+}$ with a corresponding bleaching of bands of 2AP at 472 cm^{-1}, 444 cm^{-1} and 413 cm^{-1} (Fig. 4).

The lowest energy 2AP•(−H) tautomers have a proton abstracted from the amino (NH_2) group of 2-aminopurine. The calculated spectra for 2AP•(−H,N2') (Fig. 5) and 2AP•(−H,N2) (Fig. 6), show the loss of a proton from the amino group of 2AP with the bleaching of the σNH_2 band at 1604 cm^{-1}. Together, with bleaching of the in-plane ring vibration of 2AP at 1387 cm^{-1}. There are also differences between the IR spectra 2AP•(−H,N2) and 2AP•(−H,N2') where an in-plane ring transient band is observed 1329 cm^{-1} and 1344 cm^{-1}, respectively. Where bands can be compared between 2AP•(−H,N2) and 2AP, they are blue-shifted by up to 108 cm^{-1}. The bleaching of bands in the spectral region of 450 cm^{-1} is more distinct in 2AP•(−H,N2') than for 2AP•(−H,N2) which does have some low intensity ring vibrations in this region.

Loss of a proton from the C6 or C8 position of $2AP^{\bullet+}$ to give 2AP•(−H, C6) or 2AP• (−H, C8) is not expected on thermodynamic grounds. The IR spectra of 2AP•(−H,C6) and 2AP•(−H,C8) are shown in the supplementary information (Figures S2 and S3) and are very similar to the spectra of 2AP. Deprotonation from the $2AP^{\bullet+}$ amino group has been observed in previous studies [57], and is consistent with the results observed in the current work.

Calculated spectra were also determined for the 2-aminopurine radical anion ($2AP^{\bullet-}$) (Figure S4) which could potentially be formed if 2-aminopurine in the first singlet excited state (^{1}2AP*) were to oxidise guanine according to Equation I. The IR spectra of $2AP^{\bullet-}$ has generally a similar appearance with 2AP > 1200 cm^{-1}. However, < 1200 cm^{-1} the intensities of $2AP^{\bullet-}$ in-plane and out-of-plane ring vibrations have greater intensity than for 2AP, including in the bleached region of ~500 cm^{-1}. There is also a large red-shift of the (wagging) ωC6H vibration from 932 cm^{-1} in 2AP to 436 cm^{-1} in $2AP^{\bullet-}$.

$$G + {}^1\text{2AP}^* \rightarrow G^{\bullet+} + {}^1\text{2AP}^{\bullet-} \quad \text{(I)}$$

The energies of the optimised geometries of the $2AP^-(-H^+)$ anion are stabilised in the following order N2 > N2' > C8 > C6. Again, the lowest energy tautomer is where a proton has been lost from the 2AP amino group. The calculated spectra (Figs. 7 and 8) for the tautomers of $2AP^-(-H^+,N2)$ where a proton has been removed from the 2AP amino group (the N2/N2' position) has high intensity transient bands developed in the region 1414–1509 cm^{-1} and moderately intense bands in the region of 1265-1288 cm^{-1} (Figs. 7 and 8). There is a notable difference between $2AP^-(-H^+,N2')$ and $2AP^-(-H^+,N2)$ in the region where 2AP is bleached ~450 cm^{-1}. In $2AP^-(-H^+,N2')$ there is an in-plane ring vibration at 478 cm^{-1} which is comparable to a 2AP band at 472 cm^{-1}. In $2AP^-(-H^+,N2)$ there is extensive 2AP bleaching in this area similar to that observed for the other 2AP photoproducts. $2AP^-(-H^+,N2)$ also has the development of transients in the region 478–749 cm^{-1} which are absent in both 2AP and $2AP^-(-H^+,N2')$. There is little consistency in terms of which bands are blue-shifted or red-shifted between the spectra of 2AP and $2AP^-(-H^+,N2/N2')$. The magnitude of any shift is generally 2–43 cm^{-1} for $2AP^-(-H^+,N2')$ and 2–61 cm^{-1} for $2AP^-(-H^+,N2)$. The spectra for the $2AP^-(-H^+$, C8) and $2AP^-(-H^+$, C6) species are provided in the supplementary information for completeness, (Figure S5 and S6).

It has been demonstrated that the 2-aminopurine neutral radical is capable of oxidising guanine to form the guanine radical cation ($G^{\bullet+}$) according to Equation II [39,103].

$$2AP\bullet(-H) + G \rightarrow G^{\bullet+} + 2AP^-(-H^+) \quad \text{(II)}$$

The calculated IR spectra for $G^{\bullet+}$ (Fig. 9) show a general blue-shift of bands in comparison to the spectra of guanine. The amount of blue-shift seems to increase toward lower frequencies, such that the νCO vibrational stretch is blue-shifted (G → $G^{\bullet+}$) by 33 cm^{-1} (1652 cm^{-1} → 1685 cm^{-1}) and 132 cm^{-1} (436 cm^{-1} → 568 cm^{-1}) for the wagging ωN2H band (Fig. 9). The νCO vibrational stretch is a key band for the IR spectra of guanine and there is a predicted reduction, from strong to moderate, in intensity of this band. Throughout much of IR quiescent regions of guanine (~1232 cm^{-1}, ~931 cm^{-1}, ~771 cm^{-1}, and

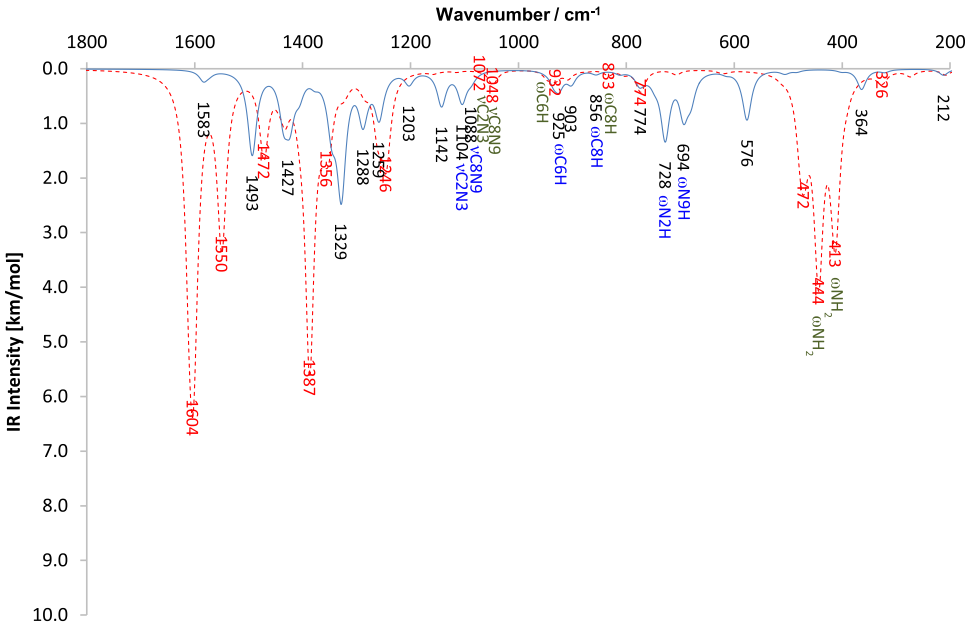

Fig. 5. Harmonic IR spectra of 2AP•(−*H*,N2') (solid blue line) and 2-aminopurine (dashed red line) calculated at B3LYP/6–31+*G*(d) level. B3LYP frequencies have been scaled by 0.9636 [72]. Annotation: *ν*, stretching; *ω*, wagging. Vibrational frequencies without annotation are in-plane (*β*ring) and out-of-plane (*γ*ring) ring vibrations. 2-Aminopurine consists of a weighted mixture of 7H–2AP (12%) and 9H–2AP (88%) and 2AP•(−*H*,N2') is a weighted mixture of 7H–2AP (<1%) and 9H–2AP (>99%).

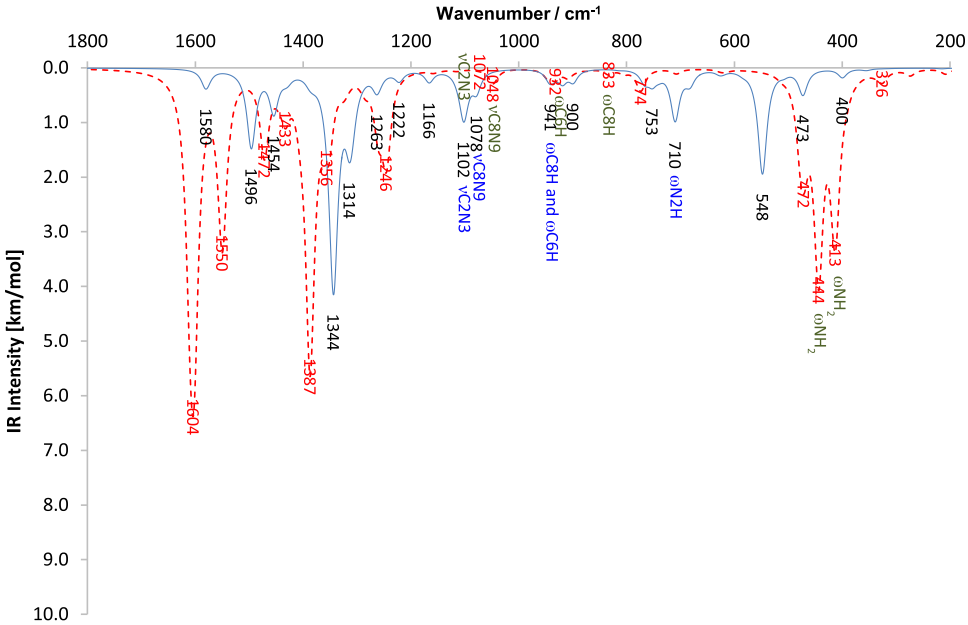

Fig. 6. Harmonic IR spectra of 2AP•(−*H*,N2) (solid blue line) and 2-aminopurine (dashed red line) calculated at B3LYP/6–31+*G*(d) level. B3LYP frequencies have been scaled by 0.9636 [72]. Annotation: *ν*, stretching; *ω*, wagging. Vibrational frequencies without annotation are in-plane (*β*ring) and out-of-plane (*γ*ring) ring vibrations. 2-Aminopurine consists of a weighted mixture of 7H–2AP (12%) and 9H–2AP (88%) and 2AP•(−*H*,N2) is a weighted mixture of 7H–2AP (<1%) and 9H–2AP (>99%).

~568 cm^{-1}), low intensity bands of $G^{\bullet+}$ vibrational stretches and wagging modes are observed. There is a bleaching of bands of guanine in the regions of ~436 cm^{-1} and ~310 cm^{-1}.

$$G^{\bullet+} + H_2O \rightarrow G^{\bullet}(-H) + H_3O^{+} \quad \text{(III)}$$

In a pulse radiolysis study with nanosecond time resolution, Kobayashi and Tagawa [53] have reported the rate of deprotonation of $G^{\bullet+}$ (Equation III) to have a rate constant of $k = 1.8 \times 10^7\ s^{-1}$. The lifetime of $G^{\bullet+}$ is $\tau = 5.6 \times 10^{-8}$ s, and would be consistent with the rapid decay of $G^{\bullet+}$ in time-resolved infrared spectra. Kuimova et al. [132] and Parker et al. [87] in their studies of guanine identified $G^{\bullet+}$ as a transient species with a blue-shifted *ν*CO vibrational stretch centred at 1702 cm^{-1}, in comparison to the *ν*CO band of guanine centred at 1662 cm^{-1}. The predicted values of the *ν*CO vibrational stretch in **Fig. 9** show the *ν*CO stretch shifting from 1652 cm^{-1} for G to 1685 cm^{-1} in $G^{\bullet+}$, and are in excellent agreement with the observations of Kuimova et al. [132] and Parker et al. [87].

The strong *ν*CO vibrational stretch (1652 cm^{-1}) of guanine is divided into two red-shifted (by at least 104 cm^{-1}) vibrational stretches of moderate intensity in G•(−*H*,N1) (Fig. 10). Bands at lower frequencies (< 1300 cm^{-1}) show blue-shifts (G → G•(−*H*,N1)): *ν*C8N9 1057 cm^{-1} → 1087 cm^{-1}, *ω*C8H 822 cm^{-1} → 922 cm^{-1} and *δ*NH_2 305 cm^{-1} → 341 cm^{-1}. There is little change in intensity in these blue-shifted bands.

However, there is an overlap in the calculated transient spectra between a ring vibration of $G^{\bullet+}$ at 1585 cm^{-1} (Fig. 9) and a *ν*CO vibrational stretch of G•(−*H*,N1) at 1587 cm^{-1} (Fig. 10), therefore making the unequivocal assignment of G•(−*H*,N1) as a photoproduct difficult.

The *ν*CO vibrational stretch that is characteristic of guanine (1652 cm^{-1}) is hardly changed in G•(−*H*,N2) (1657 cm^{-1}) and G•(−*H*,N2') (1652 cm^{-1}) (Figures S8 and S9). The scissoring *σ*NH_2 band

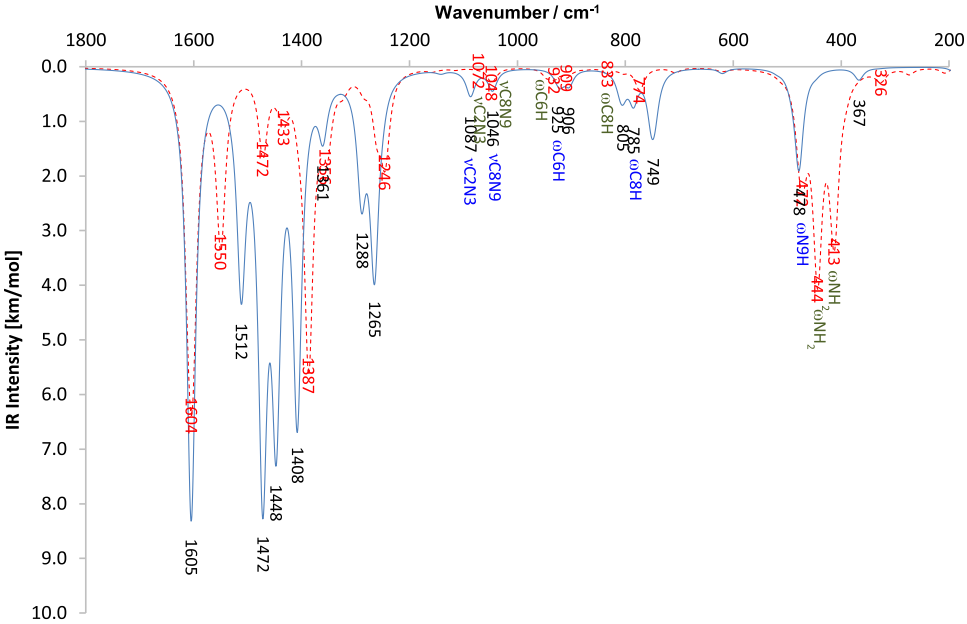

Fig. 7. Harmonic IR spectra of 2AP⁻(−*H*,N2') (solid blue line) and 2-aminopurine (dashed red line) calculated at B3LYP/6–31+*G*(d) level. B3LYP frequencies have been scaled by 0.9636 [72]. Annotation: *ν*, stretching; *ω*, wagging. Vibrational frequencies without annotation are in-plane (*β*ring) and out-of-plane (*γ*ring) ring vibrations. 2-Aminopurine consists of a weighted mixture of 7H–2AP (12%) and 9H–2AP (88%) and 2AP⁻(−*H*,N2') is a weighted mixture of 7H–2AP (<1%) and 9H–2AP (>99%).

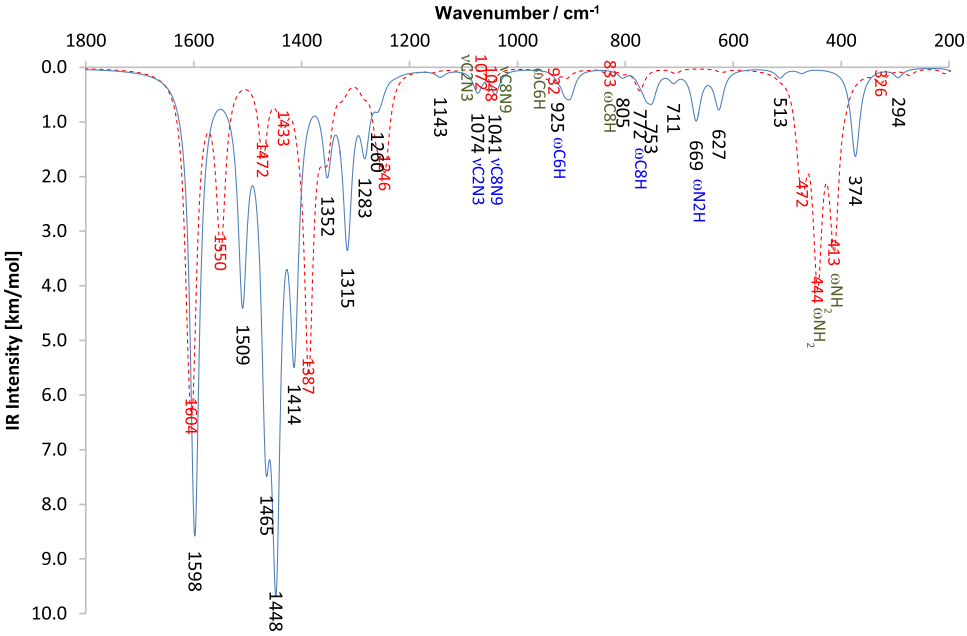

Fig. 8. Harmonic IR spectra of 2AP⁻(−*H*,N2) (solid blue line) and 2-aminopurine (dashed red line) calculated at B3LYP/6–31+*G*(d) level. B3LYP frequencies have been scaled by 0.9636 [72]. Annotation: *ν*, stretching; *ω*, wagging. Vibrational frequencies without annotation are in-plane (*β*ring) and out-of-plane (*γ*ring) ring vibrations. 2-Aminopurine consists of a weighted mixture of 7H–2AP (12%) and 9H–2AP (88%) and 2AP⁻(−*H*,N2) is a weighted mixture of 7H–2AP (<1%) and 9H–2AP (>99%).

of guanine at 1602 cm^{-1} is bleached upon loss of one of the amino group protons, as is the guanine in-plane ring vibration at 1561 cm^{-1}. In general terms the IR spectra of G•(−*H*,N2') is much closer to that of guanine than the IR spectra of G•(−*H*,N2). The region ~1400 cm^{-1} in guanine is IR quiescent, however, a low intensity transient appears at 1419 cm^{-1} in G•(−*H*,N2) (Figure S8). Further transient bands appear at 1244 cm^{-1}, 1176 cm^{-1}, 1096 cm^{-1}, 785 cm^{-1}, 543 cm^{-1} in G•(−*H*,N2) and at 1246 cm^{-1}, 1185 cm^{-1}, 1092 cm^{-1}, and 662 cm^{-1} in G•(−*H*,N2'). Two bands in guanine, the wagging *ω*N7H (447 cm^{-1}) and the in-plane ring vibration (309 cm^{-1}) are both bleached in G•(−*H*,N2), and the latter band is also bleached in G•(−*H*,N2'). However, in G•(−*H*,N2') the wagging *ω*N7H band is predicted at 440 cm^{-1} in G•(−*H*,N2'). Although their formation was not found to be thermodynamically favourable, the IR spectra of G•(−*H*,C8) is shown in the Supplementary information, Figure S10, the spectrum is very similar to that of guanine itself.

5. Conclusion

The aim of this work was to use quantum mechanical calculations (using B3LYP and EDF1 methods) to predict the thermodynamically most stable IR spectra for potential photoproducts of the one-electron oxidation of guanine by photoexcited 2-aminopurine [39,103]. The DFT calculations used were found to have excellent agreement with experimental IR spectra.

Directly comparing the IR spectra of potential photoproducts with that of 2-aminopurine or guanine, bleaching (areas of quiescent IR intensity) and the appearance of transient bands may be identified. Thermodynamic calculations have been especially useful in identifying the nature of the deprotonated 2AP•(−*H*) and G•(−*H*) neutral radicals in terms of their thermodynamic stability compared to the other deprotonated tautomers. Deprotonation of labile protons from amino or imino nitrogen of 2-aminopurine and guanine are lower in energy by

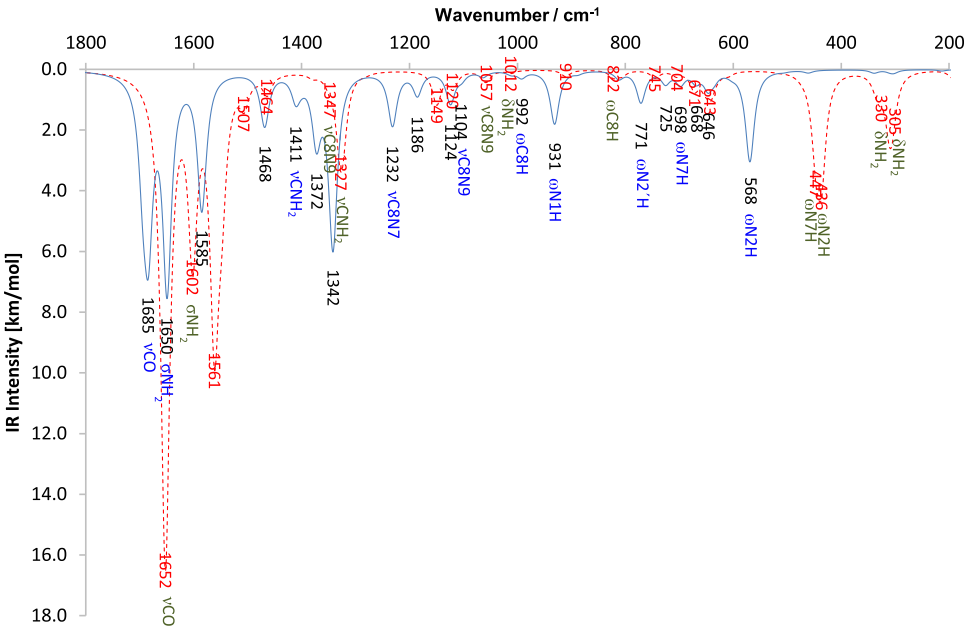

Fig. 9. Harmonic IR spectra of $G^{\bullet+}$ (solid blue line) and guanine (dashed red line) calculated at B3LYP/6–31+*G*(d) level. B3LYP frequencies have been scaled by 0.9636 [72]. Annotation: *ν*, stretching; *σ*, scissoring; *ω*, wagging; *δ*, rocking. Vibrational frequencies without annotation are in-plane (*β*ring) and out-of-plane (*γ*ring) ring vibrations.

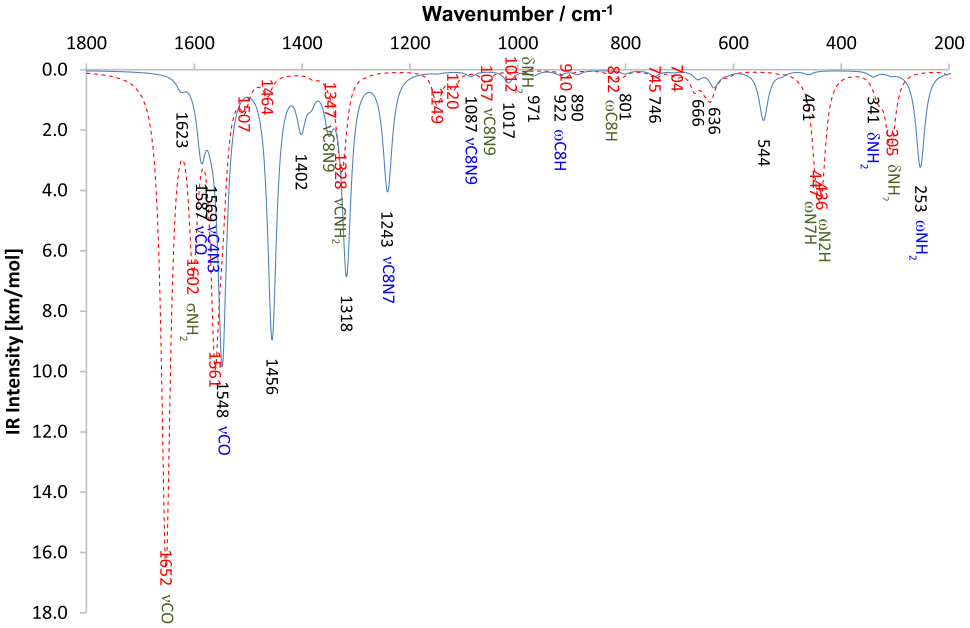

Fig. 10. Harmonic IR spectra of G•(−*H*,N1) (solid blue line) and guanine (dashed red line) calculated at B3LYP/6–31+*G*(d) level. B3LYP frequencies have been scaled by 0.9636 [72]. Annotation: *ν*, stretching; *σ*, scissoring; *ω*, wagging; *δ*, rocking. Vibrational frequencies without annotation are in-plane (*β*ring) and out-of-plane (*γ*ring) ring vibrations.

at least 8.393 kcal mol^{-1} for 2AP and by 23.667 kcal mol^{-1} for guanine than proton loss from the non-labile C6 and C8 positions. The 2AP•(−*H*,N2') and G•(−*H*,N1) deprotonated tautomers were found to be the most thermodynamically stable structures of the purine neutral radicals with G•(−*H*,N2) shown to be only marginally less stable and at equilibrium both species are expected to be present in roughly 60:40 ratio. For 2-aminopurine anions, the most thermodynamically favoured structure is proton loss from the 2AP amino group ($2AP^{-}$(−*H*,N2)). Thus, the intermediates of the reaction pathway where guanine is oxidised by photoexcited 2-aminopurine can be proposed. Biphotonic ionization (λ = 308 nm) of 2-aminopurine results in formation of the 2-aminopurine radical cation ($2AP^{\bullet+}$). Rapid deprotonation (to the bulk solvent) of $2AP^{\bullet+}$ follows with the formation of the 2-aminopurine neutral radical (2AP•(−*H*,N2')) which in turn oxidises guanine to produce the guanine radical cation ($G^{\bullet+}$) and the 2-aminopurine anion ($2AP^{-}$(−*H*,N2)). Deprotonation (to the bulk solvent) of $G^{\bullet+}$ forms a neutral guanine radical (G•(−*H*,N1)). H^{+} (from the bulk solvent) combines with ($2AP^{-}$(−*H*,N2)) to re-form 2AP. In summary, the approach of predicting IR spectra and thermodynamic properties to enable the identification of reaction intermediates is a powerful technique that can greatly assist preparation prior to commencing experimental work.

Contributors

KCT designed the experiments; GDB and KCT have written the text; GDB conducted experiments and data analysis.

Data statement

The authors declare that the raw data is available under request.

Funding

We gratefully acknowledge support from the EPSRC UK NSCCS project code CHEM794.

Declaration of Competing Interest

The authors declare that they have no known competing financial interests or personal relationships that could have appeared to influence the work reported in this paper.

Acknowledgements

The authors wish to thank Dr David Houldershaw and Richard Westlake for supporting the Asgard cluster at Birkbeck.

Supplementary materials

Supplementary material associated with this article can be found, in the online version, at doi:10.1016/j.jpap.2021.100025.

References

[1] A. Adhikary, A. Kumar, D. Becker, M.D. Sevilla, The Guanine Cation Radical: Investigation of Deprotonation States by ESR and DFT, J. Phys. Chem. B 110 (2006) 24171–24180, doi:10.1021/jp064361y.
[2] A. Adhikary, D. Khanduri, M.D. Sevilla, Direct observation of the hole protonation state and hole localization site in DNA-oligomers, J. Am. Chem. Soc. 131 (2009) 8614–8619, doi:10.1021/ja9014869.
[3] A. Adhikary, A. Kumar, S.A. Munafo, D. Khanduri, M.D. Sevilla, Prototropic equilibria in DNA containing one-electron oxidized GC:intra-duplex vs. duplex to solvent deprotonation, Phys. Chem. Chem. Phys. 12 (2010) 5353–5368, doi:10.1039/b925496j.
[4] D. Angelov, A. Spassky, M. Berger, J. Cadet, High-intensity UV laser photolysis of DNA and Purine 2'-deoxyribonucleosides: formation of 8-oxopurine damage and oligonucleotide strand cleavage as revealed by HPLC and gel electrophoresis studies, J. Am. Chem. Soc. 119 (1997) 11373–11380, doi:10.1021/ja971728r.
[5] M.R. Arkin, E.D.A. Stemp, S. Coates Pulver, J.K Barton, Long-range oxidation of guanine by Ru(III) in duplex DNA, Chem. Biol. 4 (1997) 389–400, doi:10.1016/S1074-5521(97)90129-0.
[6] K.-D. Asmus, D.J. Deeble, A. Garner, K.M. Idriss Ali, G. Scholes, Chemical aspects of radiosensitization. Reaction of sensitizers with radicals produced in the radiolysis of aqueous solutions of nucleic acid components, Br. J. Cancer 37 (Suppl. III) (1978) 46–49 *Suppl. III*.
[7] V. Bachler, K. Hildenbrand, EPR-detection of the guanosyl radical cation in aqueous solution. quantum chemically supported assignment of nitrogen and proton hyperfine couplings, Radiation Phys. Chem. 40 (1992) 59–68, doi:10.1016/1359-0197(92)90141-2.
[8] A. Banyasz, E. Balanikas, L. Martinez-Fernandez, G. Baldacchino, T. Douki, R. Improta, D. Markovitsi, Radicals generated in tetramolecular guanine quadruplexes by photoionization: spectral and dynamical features, J. Phys. Chem. B 123 (2019) 4950–4957, doi:10.1021/acs.jpcb.9b02637.
[9] E. Balanikas, A. Banyasz, G. Baldacchino, D. Markovitsi, Populations and dynamics of guanine radicals in DNA strands—direct versus indirect generation, Molecules 24 (2019) 2347–2363, doi:10.3390/molecules24132347.
[10] B. Brauer, R.B. Gerber, M. Kabelac, P. Hobza, J.M. Bakker, A.G.A. Riziq, M.S De Vries, Vibrational spectroscopy of the G•••C base pair: experiment, harmonic and anharmonic calculations, and the nature of the anharmonic couplings, J. Phys. Chem. A 109 (2005) 6974–6984, doi:10.1021/jp051767m.
[11] G.V. Buxton, C.L. Greenstock, W.P. Helman, A.B. Ross, Critical review of rate constants for reactions of hydrated electrons, hydrogen atoms and hydroxyl radicals (·OH/·O−) in Aqueous Solution, J. Phys. Chem. Ref. Data 17 (1988) 513–886, doi:10.1063/1.555805.
[12] J. Cadet, T. Douki, J.-.L. Ravanat, Oxidatively generated damage to the guanine moiety of DNA: mechanistic aspects and formation in cells, Acc. Chem. Res. 41 (2008) 1075–1083, doi:10.1021/ar700245e.
[13] J. Cadet, R.J. Wagner, V. Shafirovich, N.E. Geacintov, One-electron oxidation reactions of purine and pyrimidine bases in cellular DNA, Int. J. Radiat. Biol. 90 (2014) 423–432, doi:10.3109/09553002.2013.877176.
[14] J. Cadet, K.J.A Davies, Oxidative DNA damage & repair: an introduction, Free Radic. Biol. Med. 107 (2017) 2–12, doi:10.1016/j.freeradbiomed.2017.03.030.
[15] J. Cadet, R.J. Wagner, D. Angelov, Biphotonic ionization of DNA: from model studies to cell, Photochem. Photobiol. 95 (2019) 59–72, doi:10.1111/php.13042.
[16] P.R. Callis, Electronic states and luminescence of nucleic acid systems, Annu Rev Phys Chem 34 (1983) 329–357, doi:10.1146/annurev.pc.34.100183.001553.
[17] L.P. Candeias, S. Steenken, Structure and acidbase properties of oneelectronoxidized deoxyguanosine, guanosine, and 1-methylguanosine, J. Am. Chem. Soc. 111 (1989) 1094–1099, doi:10.1021/ja00185a046.
[18] L.P. Candeias, S. Steenken, Ionization of purine nucleosides and nucleotides and their components by 193 nm laser photolysis in aqueous solution: model studies for oxidative damage of DNA, J. Am. Chem. Soc. 114 (1992) 699–704, doi:10.1021/ja00028a043.
[19] L.P. Candeias, S. Steenken, Reaction of HO• with guanine derivatives in aqueous solution: formation of two different redoxactive OH-Adduct radicals and their unimolecular transformation reactions. Properties of G(H)•, Chem. Eu. J. 6 (2000) 475–484 https://doi.org/10.1002/(SICI)1521-3765(20000204)6:3≤475::AID-CHEM475≥3.0.CO;2-E, doi:10.1002/(SICI)1521-3765(20000204)6:3<475::AID-CHEM475>3.0.CO;2-E.
[20] C. Chatgilialoglu, C. Caminal, M. Guerra, Q.G. Mulazzani, Tautomers of one-electron-oxidized guanosine, Angew. Chem. Int. Ed. 44 (2005) 6030–6032, doi:10.1002/anie.200501087.
[21] M.Y. Choi, R.E. Miller, Four tautomers of isolated guanine from infrared laser spectroscopy in helium nanodroplets, J. Am. Chem. Soc. 128 (2006) 7320–7328, doi:10.1021/ja060741l.
[22] P.M. Cullis, M.E. Malone, L.A. Merson-Davies, Guanine radical cations are precursors of 7,8-dihydro-8-oxo-2'-deoxyguanosine but are not precursors of immediate strand breaks in DNA, J. Am. Chem. Soc. 118 (1996) 2775–2781, doi:10.1021/ja9536025.
[23] J.M. Delabar, M. Majoube, Infrared and Raman spectroscopic study of ^{15}N and D-substituted guanines, Spectrochmica Acta 34A (1978) 129–140, doi:10.1016/0584-8539(78)80106-8.
[24] G.W. Doorley, D.A. McGovern, M.W. George, M. Towrie, A.W. Parker, J.M. Kelly, S.J. Quinn, Picosecond transient infrared study of the ultrafast deactivation processes of electronically excited B-DNA and Z-DNA forms of [poly(dG-dC)]$_2$, Angewandte Chem. Int. Edition 48 (2009) 123–127, doi:10.1002/anie.200803904.
[25] G.W. Doorley, M. Wojdyla, G.W. Watson, M. Towrie, A.W. Parker, J.M. Kelly, S.J. Quinn, Tracking DNA excited states by picosecond-time-resolved infrared spectroscopy: signature band for a charge-transfer excited state in stacked adenine-thymine systems, J. Phys. Chem. Lett. 4 (2013) 2739–2744, doi:10.1021/jz401258n.
[26] T. Douki, D. Angelov, J. Cadet, UV laser photolysis of DNA: effect of duplex stability on charge-transfer efficiency, J. Am. Chem. Soc. 123 (2001) 11360–11366, doi:10.1021/ja016426a.
[27] T. Douki, J.-.L. Ravanat, D. Angelov, J.R. Wagner, J. Cadet, Effects of duplex stability on charge-transfer efficiency within DNA, Top Curr Chem 236 (2004) 1–25, doi:10.1007/b94409.
[28] R. Eritja, B.E. Kaplan, D. Mhaskar, L.C. Sowers, J. Petruska, M.F. Goodman, Synthesis and properties of defined DNA oligomers containing base mispairs involving 2-aminopurine, Nucleic Acids Res. 14 (1986) 5869–5884, doi:10.1093/nar/14.14.5869.
[29] L. Feketeová, G.N. Khairallah, B. Chan, V. Steinmetz, P. Maître, L. Radom, R.A.J O'Hair, Gas-phase infrared spectrum and acidity of the radical cation of 9-methylguanine, Chem. Commun. 49 (2013) 7343–7345, doi:10.1039/C3CC43244K.
[30] L. Feketeová, B. Chan, G.N. Khairallah, V. Steinmetz, P. Maitre, L. Radom, R.A.J O'Hair, Watson-Crick base pair radical cation as a model for oxidative damage in DNA, J. Phys. Chem. Lett. 8 (2017) 3159–3165, doi:10.1021/acs.jpclett.7b01251.
[31] T. Fiebig, C. Wan, A.H. Zewail, Femtosecond charge transfer dynamics of a modified DNA base: 2-aminopurine in complexes with nucleotides, ChemPhysChem 3 (2002) 781–788 https://doi.org/10.1002/1439-7641(20020916)3:9≤781::AID-CPHC781≥3.0.CO;2-U, doi:10.1002/1439-7641(20020916)3:9<781::AID-CPHC781>3.0.CO;2-U.
[32] A.M. Fleming, C.J. Burrows, Formation and processing of DNA damage substrates for the hNEIL enzymes, Free Radic. Biol. Med. 107 (2017) 35–52, doi:10.1016/j.freeradbiomed.2016.11.030.
[33] J. Florian, J. Leszczynski, What changes occur in vibrational spectra of guanine and cytosine when they form the watson-crick base pair? A quantum chemical SCRF HF/6-31 G* Study, Int J Quantum Chem (1995) 207–225, doi:10.1002/qua.560560722.
[34] J. Florian, J. Leszczynski, B.G. Johnson, On the intermolecular vibrational-modes of the guanine ... cytosine, adenine ... Ttymine and formamide ... formamide H-bonded dimers, J Mol Struct 349 (1995) 421–426, doi:10.1016/0022-2860(95)08799-2.
[35] S.M. Gasper, G.B. Schuster, Intramolecular photoinduced electron transfer to anthraquinones linked to duplex DNA: the effect of gaps and traps on longrange radical cation migration, J. Am. Chem. Soc. 119 (1997) 12762–12771, doi:10.1021/ja972496z.
[36] J.C. Genereux, M.W. Wuerth, J.K. Barton, Single-step charge transport through DNA over long distances, J. Am. Chem. Soc. 133 (2011) 3863–3868, doi:10.1021/ja107033v.
[37] B. Giese, Long-distance electron transfer through DNA, Annu. Rev. Biochem. 71 (2002) 51–70, doi:10.1146/annurev.biochem.71.083101.134037.
[38] I.R. Gould, M.A. Vincent, I.H. Hillier, A theoretical-study of the infrared-spectra of guanine tautomers, Spectrochimica Acta Part A-Mol. Biomole. Spectroscopy 49 (1993) 1727–1734, doi:10.1016/0584-8539(93)80240-B.
[39] D.B. Hall, R.E. Holmlin, J.K. Barton, Oxidative DNA damage through longrange electron transfer, Nature 382 (1996) 731–735, doi:10.1038/382731a0.
[40] M.A. Harris, A.K. Mishra, R.M. Young, K.E. Brown, M.R. Wasielewski, F.D. Lewis, Direct observation of the hole carriers in DNA photoinduced charge transport, J. Am. Chem. Soc. 138 (2016) 5491–5494, doi:10.1021/jacs.6b00702.
[41] E.O. Hole, W.H. Nelson, D.M. Close, E. Sagstuen, ESR and ENDOR study of the guanine cation: secondary product in 5'•dGMP, J. Chem. Phys. 86 (1987) 5218–5219, doi:10.1063/1.452647.

[42] A. Holmén, B. Norden, B. Albinsson, Electronic transition moments of 2-aminopurine, J. Am. Chem. Soc. 119 (1997) 3114–3121, doi:10.1021/ja9635600.

[43] N.S. Hush, A.S. Cheung, Ionization potentials and donor properties of nucleic acid bases and related compounds, Chem. Phys. Lett. 35 (1975) 11–13, doi:10.1016/0009-2614(75)80190-4.

[44] M. Hutter, T. Clark, On the enhanced stability of the guanine-cytosine base-pair radical cation, J. Am. Chem. Soc. 118 (1996) 7574–7577 https://doi.org/10.1021/ja953370, doi:10.1021/ja953370.

[45] K. Ito, S. Inoue, K. Yamamoto, S. Kawanishi, 8-Hydroxydeoxyguanosine formation at the 5′ site of 5′-GG-3′ sequences in double-stranded DNA by UV radiation with riboflavin, J. Biol. Chem. 268 (1993) 13221–13227.

[46] J.M. Jean, K.B. Hall, 2-Aminopurine electronic structure and fluorescence properties in DNA, Biochemistry 41 (2002) 13152–13161, doi:10.1021/bi020308y.

[47] H. Kasai, Z. Yamaizumi, Photosensitized formation of 7,8-dihydro-8-oxo-2'-deoxyguanosine (8-hydroxy-2′-deoxyguanosine) in DNA by riboflavin: a non singlet oxygen mediated reaction, J. Am. Chem. Soc. 114 (1992) 9692–9694, doi:10.1021/ja00050a078.

[48] S. Kawanishi, Y. Hiraku, S. Oikawa, Mechanism of guanine-specific DNA damage by oxidative stress and its role in carcinogenesis and aging, Mutat. Res. 488 (2001) 65–76, doi:10.1016/S1383-5742(00)00059-4.

[49] P.M. Keane, M. Wojdyla, G.W. Doorley, G.W. Watson, I.P. Clark, G.M. Greetham, A.W. Parker, M. Towrie, J.M. Kelly, S.J. Quinn, A comparative picosecond transient infrared study of 1-methylcytosine and 5 '-dCMP that sheds further light on the excited states of cytosine derivatives, J. Am. Chem. Soc. 133 (2011) 4212–4215, doi:10.1021/ja1106089.

[50] P.M. Keane, F.R. Baptista, S.P. Gurung, S.J. Devereux, I.V. Sazanovich, M. Towrie, J.A. Brazier, C.J. Cardin, J.M. Kelly, S.J. Quinn, Long-lived excited-state dynamics of i-motif structures probed by time-resolved infrared spectroscopy, ChemPhysChem 17 (2016) 1281–1287, doi:10.1002/cphc.201501183.

[51] S.O. Kelley, J.K. Barton, Electron transfer between bases in double helical DNA, Science 283 (1999) 375–381, doi:10.1126/science.283.5400.375.

[52] S.O. Kelley, E.M. Boon, J.K. Barton, N.M. Jackson, M.G. Hill, Single-base mismatch detection based on charge transduction through DNA, Nucleic Acids Res. 27 (1999) 4830–4837, doi:10.1093/nar/27.24.4830.

[53] K. Kobayashi, S. Tagawa, Direct observation of guanine radical cation deprotonation in duplex DNA using pulse radiolysis, J. Am. Chem. Soc. 125 (2003) 10213–10218, doi:10.1021/ja036211w.

[54] K. Kobayashi, R. Yamagami, S. Tagawa, Effect of base sequence and deprotonation of guanine cation radical in DNA, J. Phys. Chem. B 112 (2008) 10752–19757, doi:10.1021/jp804005t.

[55] M. Kondo, J. Nappa, K.L. Ronayne, A.L. Stelling, P.J. Tonge, S.R. Meech, Ultrafast vibrational spectroscopy of the flavin chromophore, J. Phys. Chem. B 110 (2006) 20107–20110, doi:10.1021/jp0650735.

[56] M.K. Kuimova, J. Dyer, M.W. George, D.C. Grills, J.M. Kelly, P. Matousek, A.W. Parker, X.Z. Sun, M. Towrie, A.M. Whelan, Monitoring the effect of ultrafast deactivation of the electronic excited states of DNA bases and polynucleotides following 267 nm laser excitation using picosecond time-resolved infrared spectroscopy, Chem. Commun. (2005) 1182–1184, doi:10.1039/B414450C.

[57] M.K. Kuimova, P.M.W. Gill, C.Y. Lin, P. Matousek, M. Towrie, X.Z. Sun, M.W. George, A.W Parker, Picosecond TimeResolved Infrared Study of 2Aminopurine Ionization in Solution, Photochem. Photobiol. Sci. 6 (2007) 949–955, doi:10.1039/B705801B.

[58] A. Kumar, M.D. Sevilla, Excited states of one-electron oxidized guanine-cytosine base pair radicals: a time dependent density functional theory study, J. Phys. Chem. A 123 (2019) 3098–3108, doi:10.1021/acs.jpca.9b00906.

[59] O.F.A. Larsen, I.H.M. van Stokkum, B. Gobets, R. van Grondelle, H van Amerongen, Probing the structure and dynamics of a DNA hairpin by ultrafast quenching and fluorescence depolarization, Biophys. J. 81 (2001) 1115–1126, doi:10.1016/S0006-3495(01)75768-2.

[60] O.F.A. Larsen, I.H.M. van Stokkum, F.L. de Weerd, M. Vengris, C.T. Aravindakumar, R. van Grondelle, N.E. Geacintov, H van Amerongenc, Ultrafast transient-absorption and steady-state fluorescence measurements on 2-aminopurine substituted dinucleotides and 2-aminopurine substituted DNA duplexes, Phys. Chem. Chem. Phys. 6 (2004) 154–160, doi:10.1039/B308992D.

[61] A. Latus, M.S. Alam, M. Mostafavi, J.-.L. Marignier, E Maisonhaute, Guanosine radical reactivity explored by pulse radiolysis coupled with transient electrochemistry, Chem. Commun. 44 (2015) 9089–9092, doi:10.1039/C5CC02211H.

[62] Y.A. Lee, A. Durandin, P.C. Dedon, E. Nicholas, N.E. Geacintov, V. Shafirovich, Oxidation of guanine in G, GG, and GGG sequence contexts by aromatic pyrenyl radical cations and carbonate radical anions: relationship between kinetics and distribution of alkali-labile lesions, J. Phys. Chem. B 112 (2008) 1834–1844, doi:10.1021/jp076777x.

[63] A. Liska, I. Triskova, J. Ludvik, L. Trnkova, Oxidation potentials of guanine, guanosine and guanosine-5'-monophosphate: theory and experiment, Electrochim. Acta 318 (2019) 108–119, doi:10.1016/j.electacta.2019.06.052.

[64] S. Lobsiger, R.K. Sinha, S. Leutwyler, Building up water-wire clusters: isomer-selective ultraviolet and infrared spectra of jet-cooled 2-aminopurine $(H_2O)_n$, n=2 and 3, J. Phys. Chem. B 117 (2013) 12410–12421, doi:10.1021/jp407127c.

[65] R.P. Lopes, M. Paula, M.P.M Marques, R. Valero, J. Tomkinson, L.A.E. Batista de Carvalho, Guanine: a combined study using vibrational spectroscopy and theoretical methods, Int. J. Spectrosc. 27 (2012) 273–292, doi:10.1155/2012/168286.

[66] P. Manoj, H. Mohan, J.P. Mittal, V.M. Manoj, C.T. Aravindakumar, Charge transfer from 2-aminopurine radical cation and radical anion to nucleobases: a pulse radiolysis study, Chem. Phys. 331 (2007) 351–358, doi:10.1016/j.chemphys.2006.11.005.

[67] D.A. McGovern, S. Quinn, G.W. Doorley, A.M. Whelan, K.L. Ronayne, M. Towrie, A.W. Parker, J.M. Kelly, Picosecond infrared probing of the vibrational spectra of transients formed upon UV excitation of stacked G-tetrad structures, Chem. Commun. (2007) 5158–5160, doi:10.1039/B711172J.

[68] D.A. McGovern, G.W. Doorley, A.M. Whelan, A.W. Parker, M. Towrie, J.M. Kelly, S.J. Quinn, A study of the pH dependence of electronically excited guanosine compounds by picosecond time-resolved infrared spectroscopy, Photochem. Photobiol. Sci. 8 (2009) 542–548, doi:10.1039/B817756B.

[69] C.M. Marian, The guanine tautomer puzzle: quantum chemical investigation of ground and excited states, J. Phys. Chem. A 111 (2007) 1545–1553, doi:10.1021/jp068620v.

[70] T. Melvin, S. Cunniffe, D. Papworth, T. Roldan-Arjona, P O'Neill, Irradiation of DNA with 193 nm light yields formamidopyrimidine-DNA glycosylase (Fpg) protein-sensitive lesions, Photochem. Photobiol. 65 (1997) 660–665, doi:10.1111/j.1751-1097.1997.tb01908.x.

[71] T. Melvin, S.M.T. Cunniffe, P. O'Neill, A.W. Parker, T. Roldan-Arjona, Guanine is the target for direct ionization damage in DNA, as detected using excision enzymes, Nucleic Acids Res. 26 (1998) 4935–4942, doi:10.1093/nar/26.21.4935.

[72] J.P. Merrick, D. Moran, L. Radom, An evaluation of harmonic vibrational frequency scale factors, J. Phys. Chem. A 111 (2007) 11683–11700, doi:10.1021/jp073974n.

[73] R. Misiaszek, C. Crean, A. Joffe, N.E. Geacintov, V. Shafirovich, Oxidative DNA damage associated with combination of guanine and superoxide radicals and repair mechanisms via radical trapping, J. Biol. Chem. 279 (2004) 32106–32115, doi:10.1074/jbc.M313904200.

[74] M. Mons, I. Dimicoli, F. Piuzzi, B. Tardivel, M. Elhanine, Tautomerism of the DNA base guanine and its methylated derivatives as studied by gas-phase infrared and ultraviolet spectroscopy, J. Phys. Chem. A 106 (2002) 5088–5094, doi:10.1021/jp0139742.

[75] R.K. Neely, S.W. Magennis, D.T.F. Dryden, A.C Jones, Evidence of tautomerism in 2-aminopurine from fluorescence lifetime measurements, J. Phys. Chem. B 108 (2004) 17606–17610, doi:10.1021/jp0490857.

[76] R.K. Neely, S.W. Magennis, S. Parsons, A.C. Jones, Photophysics and X-ray structure of crystalline 2-aminopurine, ChemPhysChem 8 (2007) 1095–1102, doi:10.1002/cphc.200600593.

[77] D.N. Nikogosyan, V.S. Letokhov, Nonlinear laser photophysics, photochemistry and photobiology of nucleic acids, Riv. Nuovo Cimento 6 (1983) 1–72, doi:10.1007/BF02740898.

[78] E. Nir, C. Plutzer, K. Kleinermanns, M. De Vries, Properties of isolated DNA bases, base pairs and nucleosides examined by laser spectroscopy, Eu. Phys. J. D 20 (2002) 317–329, doi:10.1140/epjd/e2002-00167-2.

[79] Y. Nishimura, M. Tsuboi, S. Kato, K. Morokuma, In-plane vibrational-modes of guanine from an ab initio MO calculation, Bull. Chem. Soc. Jpn. 58 (1985) 638–645, doi:10.1246/bcsj.58.638.

[80] P. O'Neill, A.W. Parker, M.A. Plumb, L.D.A Siebbeles, Guanine modifications following ionization of DNA occurs predominantly via intra- and not interstrand charge migration: an experimental and theoretical study, J. Phys. Chem. B 105 (2001) 5283–5290, doi:10.1021/jp003514t.

[81] M.A. O'Neill, J.K. Barton, 2-aminopurine: a probe of structural dynamics and charge transfer in DNA and DNA:RNA hybrids, J. Am. Chem. Soc. 124 (2002) 13053–13066, doi:10.1021/ja0208198.

[82] M. A. O' Neill, J. K. Barton, Effects of strand and directional asymmetry on basebase coupling and charge transfer in double-helical DNA, Proceedings of the National Academy of Sciences of the United States of America 99 (2002) 16543–16550, doi:10.1073/pnas .012669599.

[83] M.A. O'Neill, H.-.C. Becker, C. Wan, J.K. Barton, A.H. Zewail, Ultrafast dynamics in DNA-mediated electron transfer: base gating and the role of temperature, Angew. Chem. Int. Ed. 42 (2003) 5896–5900, doi:10.1002/anie.200352831.

[84] M.A. O'Neill, J.K. Barton, DNA-mediated charge transport requires conformational motion of the DNA bases: elimination of charge transport in rigid glasses at 77 K, J. Am. Chem. Soc. 126 (2004) 13234–13235, doi:10.1021/ja0455897.

[85] M.A. O'Neill, J.K. Barton, DNA charge transport: conformationally gated hopping through stacked domains, J. Am. Chem. Soc. 126 (2004) 11471–11483, doi:10.1021/ja048956n.

[86] V.M. Orlov, A.N. Smirnov, Y.M. Varshavsky, Ionization potentials and electron-donor ability of nucleic acid bases and their analogues, Tetrahedron Lett. 48 (1976) 4377–4378, doi:10.1016/0040-4039(76)80120-7.

[87] A.W. Parker, C.Y. Lin, M.W. George, M. Towrie, M.K. Kuimova, Infrared characterization of the guanine radical cation: finger printing DNA damage, J. Phys. Chem. B 114 (2010) 3660–3667, doi:10.1021/jp9106958.

[88] F.E. Poynton, J.P. Hall, P.M. Keane, C. Schwarz, I.V. Sazanovich, M. Towrie, T. Gunnlaugsson, C.J. Cardin, D.J. Cardin, S.J. Quinn, C. Long, J.M. Kelly, Direct observation by time-resolved infrared spectroscopy of the bright and the dark excited states of the $[Ru(phen)_2(dppz)]^{2+}$ light-switch compound in solution and when bound to DNA, Chem. Sci. 7 (2016) 3075–3084, doi:10.1039/C5SC04514B.

[89] F. Prat, K.N. Houk, C.S. Foote, Effect of guanine stacking on the oxidation of 8-oxoguanine in B-DNA, J. Am. Chem. Soc. 120 (1998) 845–846, doi:10.1021/ja972331q.

[90] E.L. Rachofsky, R. Osman, J.B.A Ross, Probing structure and dynamics of DNA with 2-aminopurine: effects of local environment on fluorescence, Biochemistry 40 (2001) 946–956, doi:10.1021/bi001664o.

[91] R. Ramaekers, L. Adamowicz, G. Maes, Tautomery and H-bonding characteristics of 2-aminopurine: a combined experimental and theoretical study, Eu. Phys. J. D 20 (2002) 375–388, doi:10.1140/epjd/e2002-00160-9.

[92] B. Rakvin, J.N. Herak, K. Voit, J. Hüttermann, Free radicals from single crystals of deoxyguanosine 5′-monophosphate (Na Salt) irradiated at low temperatures, Radiat. Environ. Biophys. 26 (1987) 1–12, doi:10.1007/BF01211360.

[93] M.J. Rist, J.P. Marino, Fluorescent nucleotide base analogs as probes of nucleic acid structure, dynamics and interactions, Curr. Org. Chem. 6 (2002) 775–793, doi:10.2174/1385272023373914.
[94] Y. Rokhlenko, N.E. Geacintov, V. Vladimir Shafirovich, Lifetimes and reaction pathways of guanine radical cations and neutral guanine radicals in an oligonucleotide in aqueous solutions, J. Am. Chem. Soc. 134 (2012) 4955–4962, doi:10.1021/ja212186w.
[95] Y. Rokhlenko, J. Cadet, N.E. Geacintov, V. Vladimir Shafirovich, Mechanistic aspects of hydration of guanine radical cations in DNA, J. Am. Chem. Soc. 136 (2014) 5956–5962, doi:10.1021/ja412471u.
[96] I. Saito, M. Takayama, H. Sugiyama, K. Nakatani, Photoinduced DNA cleavage via electron transfer: demonstration that guanine residues located 5' to guanine are the most electron-donating sites, J. Am. Chem. Soc. 117 (1995) 6406–6407, doi:10.1021/ja00128a050.
[97] I. Saito, T. Nakamura, K. Nakatani, Y. Yoshioka, K. Kizashi Yamaguchi, K. Sugiyama, Mapping of the hot spots for DNA damage by one-electron oxidation: efficacy of GG Doublets and GGG triplets as a trap in long-range hole migration, J. Am. Chem. Soc. 120 (1998) 12686–12687, doi:10.1021/ja981888i.
[98] M.W. Schmidt, K.K. Baldridge, J.A. Boatz, S.T. Elbert, M.S. Gordon, J.H. Jensen, S. Koseki, N. Matsunaga, K.A. Nguyen, S.J. Su, T.L. Windus, M. Dupuis, J.A. Montgomery, General atomic and molecular electronicstructure system, J. Comput. Chem. 14 (1993) 1347–1363, doi:10.1002/jcc.540141112.
[99] K.A. Seefeld, C. Plutzer, D. Lowenich, T. Haber, R. Linder, K. Kleinermanns, J. Tatchen, C.M. Marian, Tautomers and electronic states of jet-cooled 2-aminopurine investigated by double resonance spectroscopy and theory, Phys. Chem. Chem. Phys. 7 (2005) 3021–3026, doi:10.1039/B505954B.
[100] C.A.M. Seidel, A. Schulz, M.H.M Sauer, Nucleobase specific quenching of fluorescent dyes. 1. Nucleobase one-electron redox potentials and their correlation with static and dynamic quenching efficiencies, J. Phys. Chem. 100 (1996) 5541–5553, doi:10.1021/jp951507c.
[101] K. Senthilkumar, F.C. Grozema, C. Fonseca Guerra, F.M. Bickelhaupt, L.D.A Siebbeles, Mapping the sites for selective oxidation of guanines in DNA, J. Am. Chem. Soc. 125 (2003) 13658–13659, doi:10.1021/ja037027d.
[102] M.D. Sevilla, D. Becker, M. Yan, S.R. Summerfield, Relative abundances of primary ion radicals in γ-irradiated DNA: cytosine vs thymine anions and guanine vs adenine cations, J. Phys. Chem. 95 (1991) 3409–3415, doi:10.1021/j100161a080.
[103] V. Shafirovich, A. Dourandin, W.D. Huang, N.P. Luneva, N.E. Geacintov, Oxidation of guanine at a distance in oligonucleotides induced by twophoton photoionization of 2-aminopurine, J. Phys. Chem. B 103 (1999) 10924–10933, doi:10.1021/jp992002f.
[104] V. Shafirovich, A. Dourandin, N.P. Luneva, N.E. Geacintov, Acid–base equilibria in aqueous solutions of 2-aminopurine radical cations generated by two-photon photoionization, J. Chem. Soc. Perkin Trans. 2 (2000) (2000) 271–275, doi:10.1039/A907995E.
[105] V. Shafirovich, A. Dourandin, N.P. Luneva, N.E. Geacintov, The kinetic deuterium isotope effect as a probe of a proton coupled electron transfer mechanism in the oxidation of guanine by 2-aminopurine radicals, J. Phys. Chem. B 104 (2000) 137–139, doi:10.1021/jp993239e.
[106] V. Shafirovich, A. Dourandin, W.D. Huang, N.P. Luneva, N.E. Geacintov, Electron transfer at a distance induced by siteselective photoionization of 2-aminopurine in oligonucleotides and investigated by transient absorption techniques, Phys. Chem. Chem. Phys. 2 (2000) 4399–4408, doi:10.1039/B004896H.
[107] V. Shafirovich, A. Dourandin, W. Huang, N.E. Geacintov, The carbonate radical is a site-selective oxidizing agent of guanine in double-stranded oligonucleotides, J. Biol. Chem. 276 (2001) 24621–24626 https://do.org/10.1074/jbc.M101131200, doi:10.1074/jbc.M101131200.
[108] V. Shafirovich, A. Dourandin, N.E. Geacintov, Proton-coupled electrontransfer reactions at a distance in DNA duplexes: kinetic deuterium isotope effect, J. Phys. Chem. B 105 (2001) 8431–8435, doi:10.1021/jp0044734.
[109] R. Singh, R.A. Yadav, Vibrational investigations of guanine, thioguanine and their singly charged cations and anions, Indian J. Phys. 91 (2017) 71–92, doi:10.1007/s12648-016-0877-y.
[110] R.K. Sinha, S. Lobsiger, M. Trachsel, S. Leutwyler, Vibronic spectra of jet-cooled 2-aminopurine•H_2O clusters studied by UV resonant two-photon ionization spectroscopy and quantum chemical calculations, J. Phys. Chem. A 115 (2011) 6208–6217, doi:10.1021/jp111469n.
[111] R.K. Sinha, S. Lobsiger, S. Leutwyler, Isomer- and species-selective infrared spectroscopy of jet-cooled 7H- and 9H-2-aminopurine and 2-aminopurine•H_2O clusters, J. Phys. Chem. A 116 (2012) 1129–1136, doi:10.1021/jp2077177.
[112] J. Smagowicz, K.L. Wierzchowski, Lowest excited states of 2-aminopurine, J. Lumin. 8 (1974) 210–232, doi:10.1016/0022-2313(74)90057-X.
[113] O.J.G. Somsen, A. van Hoek, H van Amerongen, Fluorescence quenching of 2-aminopurine in dinucleotides, Chem. Phys. Lett. 402 (2005) 61–65, doi:10.1016/j.cplett.2004.11.122.
[114] L.C. Sowers, Y. Boulard, G.V. Fazakerley, Multiple structures for the 2-aminopurine-cytosine mispair, Biochemistry 39 (2000) 7613–7620, doi:10.1021/bi992388k.
[115] S. Steenken, Purine bases, nucleosides, and nucleotides: aqueous solution redox chemistry and transformation reactions of their radical cations and e^- and OH adducts, Chem. Rev. 89 (1989) 503–520, doi:10.1021/cr00093a003.
[116] S. Steenken, J.P. Telo, H.M. Novais, L.P. Candeias, One-electron-reduction potentials of pyrimidine bases, nucleosides, and nucleotides in aqueous solution. consequences for DNA redox chemistry, J. Am. Chem. Soc. 114 (1992) 4701–4709, doi:10.1021/ja00038a037.
[117] S. Steenken, Electron transfer in DNA? Competition by ultra-fast proton transfer? Biol. Chem. 378 (1997) 1293–1297.
[118] S. Steenken, S.V. Jovanovic, OneElectron reduction potentials of adenosine and guanosine radicals in aqueous solution, J. Am. Chem. Soc. 119 (1997) 617–618, doi:10.1021/ja962255b.
[119] E.D.A. Stemp, M.R. Arkin, J.K Barton, Oxidation of guanine in DNA by Ru(phen)2(dppz)$^{3+}$ using the flash-quench technique, J. Am. Chem. Soc. 119 (1997) 2921–2925, doi:10.1021/ja963606p.
[120] K. Szczepaniak, M. Szczesniak, Matrix isolation infrared studies of nucleic acid constituents, J. Mol. Struct. 156 (1987) 29–42, doi:10.1016/0022-2860(87)85038-X.
[121] U. Thewalt, C.E. Bugg, R.E. Marsh, The crystal structure of guanine monohydrate, Acta Crystallogr. B27 (1971) 2358–2363, doi:10.1107/S0567740871005880.
[122] M. Towrie, G.W. Doorley, M.W. George, A.W. Parker, S.J. Quinn, J.M. Kelly, ps-TRIR covers all the bases - recent advances in the use of transient IR for the detection of short-lived species in nucleic acids, Analyst 134 (2009) 1265–1273, doi:10.1039/B902108F.
[123] D. Voet, W.B. Gratzer, R.A. Cox, P. Doty, Absorption spectra of nucleotides, polynucleotides, and nucleic acids in the far ultraviolet, Biopolymers 1 (1963) 193–208, doi:10.1002/bip.360010302.
[124] Y. Wang, H. Zhao, Q. Zhou, X. Dai, K. Kunhui Liu, D. Song, H. Su, Monitoring the structure-dependent reaction pathways of guanine radical cations in triplex DNA: deprotonation versus hydration, J. Phys. Chem. B 123 (2019) 2853–2863, doi:10.1021/acs.jpcb.9b00608.
[125] D.C. Ward, E. Reich, L. Stryer, Fluorescence studies of nucleotides and polynucleotides. I. formycin, 2-aminopurine riboside, 2,6-diaminopurine riboside, and their derivatives, J. Biol. Chem. 244 (1969) 1228–1237.
[126] L. Wu, K. Liu, J. Jie, D. Song, H. Su, Direct observation of guanine radical cation deprotonation in G-quadruplex DNA, J. Am. Chem. Soc. 137 (2015) 259–266, doi:10.1021/ja510285t.
[127] J.D. Zhang, Y. Xie, H.F. Schaefer III, Successive attachment of electrons to protonated guanine: $(G+H)^\bullet$ radicals and $(G+H)^-$ anions, J. Phys. Chem. A 110 (2006) 12010–12016, doi:10.1021/jp0634454.
[128] L. Feketeová, B. Chan, G. N. Khairallah, V. Steinmetz, P. Maitre, L. Radom, R. A. J. O'Hair, Gas-phase structure and reactivity of the keto tautomer of the deoxyguanosine radical cation, Phys. Chem. Chem. Phys. 17 (2015) 25837–25844, doi:10.1039/C5CP01573A.
[129] M. A. O'Neill, C. Dohno, J. K. Barton, Direct Chemical Evidence for Charge Transfer between Photoexcited 2-Aminopurine and Guanine in Duplex, J. Am. Chem. Soc. 126 (2004) 1316–1317, doi:10.1021/ja037802p.
[130] Y. Zhang, J. Dood, A. A. Beckstead, X. B. Li, K. V. Nguyen, C. V. Burrows, I. Roberto, B. Kohler, Photoinduced Electron Transfer in DNA: Charge Shift Dynamics Between 8-Oxo-Guanine Anion and Adenine, J. Phys. Chem. B 119 (2015) 7491–7502, doi:10.1021/jp511220x.
[131] P. M. Hare, C. T. Middleton, K. I. Mertel, J. M. Herbert, B. Kohler, Time-resolved infrared spectroscopy of the lowest triplet state of thymine and thymidine, Chem. Phys. 347 (2008) 383–392, doi:10.1016/j.chemphys.2007.10.035.
[132] M.K. Kuimova, A.J. Cowan, P. Matousek, A.W. Parker, X.Z. Sun, M. Towrie, M.W. George, Monitoring the direct and indirect damage of DNA bases and polynucleotides by using timeresolved infrared spectroscopy, Proceedings of the National Academy of Sciences of the United States of America 103 (2006) 2150–2153, doi:10.1073/pnas.0506860103.
[133] C. Wan, T. Fiebig, O. Schiemann, J.K. Barton, A.H. Zewail, Femtosecond direct observation of charge transfer between bases in DNA, Proceedings of the National Academy of Sciences of the United States of America 97 (2000) 14052–14055, doi:10.1073/pnas. 250483297.
[134] D. B. Bucher, A. Schlueter, T. Carell, W. Zinth, Watson–Crick base pairing controls excited-state decay in natural DNA, Angew. Chem. Int. Ed. 53 (2014) 11366–11369, doi:10.1002/anie.201406286.